

UC Office of the President

Research Grants Program Office (RGPO) Funded Publications

Title

Method for estimating the volatility of aerosols using the piezobalance: Examples from vaping e-cigarette and marijuana liquids

Permalink

<https://escholarship.org/uc/item/2vd7v9s4>

Authors

Wallace, Lance A
Ott, Wayne R
Cheng, Kai-Chung
et al.

Publication Date

2021-05-01

DOI

10.1016/j.atmosenv.2021.118379

Peer reviewed

1
2
3
4
5
6
7
8
9
10
11
12
13
14
15
16
17
18
19
20
21

**Method for estimating the volatility of aerosols using the Piezobalance:
examples from vaping e-cigarette and marijuana liquids**

Running title: Method for estimating volatility of aerosols

**Lance A. Wallace*¹, Wayne R. Ott², Kai-Chung Cheng², Tongke Zhao², and Lynn
Hildemann²**

**¹Independent researcher
428 Woodley Way
Santa Rosa, CA 95409
lwallace73@gmail.com**

**²Civil and Environmental Engineering Dept.
Stanford University
Palo Alto, CA**

Keywords: volatility, aerosol, Piezobalance, vaping, e-cigarettes, marijuana

22

23 **Abstract**

24

25 We present a new method to estimate the fraction of an aerosol mixture that is volatile, as well as
26 the time required for evaporation from a collecting surface. The method depends on an
27 instrument (the Piezobalance) designed to measure the accumulated mass on a quartz crystal that
28 can also measure the subsequent loss of mass due to evaporation. Commercially available e-
29 liquids or marijuana liquids were heated using an e-cigarette device or a vapor pen, inhaled, and
30 exhaled into a closed unventilated room (volume = 43 and 33 m³) in each of two residences.
31 From a set of 88 measurements on an e-liquid containing 99.7% “vegetable glycerin” (VG), we
32 estimate the fraction of the e-cigarette aerosol that is volatile to be 88% (95% confidence interval
33 (CI) 77-99%). We also estimate the time to reach 95% of the total loss of the volatile material
34 from the crystal to be 47 minutes (CI 33-60 minutes). For pure propylene glycol (PG) liquid, we
35 measured extremely high rates of evaporation, finding that the exhaled plume did not create high
36 exposures beyond about 0.65 m distance. From 124 experiments on three types of marijuana
37 cartridges, the corresponding estimates of the volatile fraction of exhaled marijuana aerosol were
38 normally 5-7% for liquids heated to moderate temperatures ($N = 106$), but 25-34% for liquids
39 heated to high temperatures ($N = 18$). In the latter case, the time to reach 95% of the total loss of
40 volatile material was on the order of 5-10 hours. This indicates the importance of volatility
41 considerations in affecting exposure to indoor aerosols from these two common sources.
42 Secondhand exposures to PM_{2.5} from e-cigarette aerosols are likely to be short-lived for most
43 scenarios, whereas we show that secondhand PM_{2.5} exposures from marijuana vaping aerosols
44 can be substantial and long-lived after a single puff.

45

46 **Practical implications**

47

48 The method presented here is general and can be used on almost any aerosol mixtures. It has the
49 advantage of requiring a single instrument that can measure both the source strength and decay
50 rates of the aerosol created by the source and also the fraction of collected material that is
51 volatile. The method identified a major difference in the expected exposure to e-cigarettes vs.
52 marijuana aerosols from vaping. The method should be of interest to investigators who study
53 particulate air pollution and to companies that manufacture air monitoring systems. A number of
54 important sources of indoor aerosol mixtures (e.g., cooking, candle use, incense, etc.) remain to
55 be investigated for volatility effects using this method.

56

57 **1. Introduction**

58

59 Volatile aerosols present a problem to persons attempting to determine particulate matter (PM)
60 mass concentrations using the accepted gravimetric method of collection on a filter, since the
61 material partially evaporates from the filter during or after collection. A portion of both primary
62 organic aerosol (POA) emitted directly from sources and secondary organic aerosol (SOA)
63 created by photochemical processes is semivolatile (Turpin and Huntzicker 1995). A well-
64 known example is ammonium nitrate, sometimes a substantial component of ambient air PM
65 (Lunden et al., 2003). Both positive and negative artifacts can occur in ambient monitoring
66 networks using quartz fiber filters (Maimone et al., 2011). Indoor air has been shown to have

67 higher concentrations of organic aerosol than outdoor air (Hodas et al., 2012; Polidori et al.,
68 2006). Not only gravimetric methods, but also the alternative piezoelectric methods such as the
69 tapered element oscillating microbalance (TEOM) have also encountered this problem. Later
70 versions of the TEOM have developed ways to measure the amount of volatile material lost
71 during collection (Thermofisher Scientific, [https://www.thermofisher.com/order/catalog/product/
72 TEOM1405](https://www.thermofisher.com/order/catalog/product/TEOM1405)). However, the TEOM is large and expensive (>\$20K) and not an easily workable
73 method for environmental scientists engaged in studying indoor air quality or personal exposure
74 to PM. For example, it is quite bulky and is usually installed at fixed air monitoring stations,
75 unable to be moved from room to room as in normal indoor air studies. Its normal operation also
76 requires a total flow rate of 16.67 L/min compared to the 1 Lpm flow rate of the less expensive
77 piezoelectric monitor known as the Piezobalance (Kanomax USA, Inc. [https://www.kanomax-
78 usa.com/](https://www.kanomax-usa.com/)) with a concomitant increase in noise. TEOMs equipped with a filter dynamic
79 measurement system (FDMS) require two alternating cycles, one of which uses clean air passed
80 across a filter to determine the mass loss due to volatility. They also require Nafion dryers to
81 control humidity. These requirements lead to a high price tag. In contrast, the Piezobalance
82 weighs 1.8 kg (approximately 4 pounds) is easily portable and battery-operated, allowing
83 operation in any location.

84
85 Here we propose a method using the Piezobalance, which can be adapted to estimate the volatile
86 fraction of aerosols of any composition. We illustrate the method using Piezobalances to
87 estimate the volatility of two aerosol mixtures of considerable recent interest: aerosols produced
88 from e-cigarettes and aerosols produced by marijuana liquid vaping.

89
90 Volatility of these aerosols is of interest, particularly if evaporation from filters could affect
91 gravimetric measurements. We consider two modes of volatility:

92
93 1) While airborne, particle numbers may change according to at least three loss mechanisms: air
94 exchange, deposition, and evaporation. The first two mechanisms (usually denoted by $a + k$) are
95 generally considered to be approximately constant over a short period of time. Evaporation
96 rates, however, may increase over time. This would appear as an increase in the decay rate,
97 which can be detected by optical monitors as we illustrate in this paper.

98
99 2) After collection on a filter, particles may continue to evaporate. The rate of evaporation can
100 be estimated by monitoring the filter mass continuously, which is possible using the
101 Piezobalance.

102 103 **1.1 Electronic cigarettes**

104
105 Electronic cigarettes (e-cigarettes) are gaining rapidly in use worldwide. They offer a way to
106 reduce dependence on tobacco cigarettes by providing nicotine but without creating combustion
107 particles responsible for most of the cardiovascular and cardiorespiratory mortality of cigarette
108 smokers. This has led to a recommendation in the UK that doctors advise smokers of the
109 potential life-saving effects of e-cigarettes (Royal College of Physicians, 2016). Some studies
110 estimate reductions in mortality of some millions of cases over the next 40 years (Levy et al.,
111 2018). However, there is also fear that youthful nonsmokers may develop an addiction to

112 nicotine that could lead to smoking tobacco cigarettes. In 2018, 14%, 29%, and 34% of 16
113 million 8th, 10th, and 12th grade high school students, respectively, reported vaping nicotine
114 (Johnston et al., 2019). On September 12, 2018, the US Food and Drug Administration gave
115 notice to five companies that they need to show adherence to the laws prohibiting youth under
116 the age of 18 or 21 from buying e-cigarettes (USFDA, 2018).

117
118 Multiple studies have been performed of the composition and particle dynamics of e-cigarette
119 aerosol as emitted from an e-cigarette device. A fundamental analysis of the effects of e-
120 cigarette fluid composition on the gas-particle ratio is provided by Pankow (2017). Volatility and
121 rate of evaporation of the pure compounds is mainly controlled by their vapor pressure. The
122 vapor pressure of 100% propylene glycol at room temperature is a bit less than 0.1 mm Hg
123 (Lyondell basell [https://www.lyondellbasell.com/globalassets/documents/chemicals-technical-
124 literature/lyondellbasell-chemicals-technical-literature-vapor-pressure-of-aqueous-propylene-
125 glycol-solutions-2518.pdf](https://www.lyondellbasell.com/globalassets/documents/chemicals-technical-literature/lyondellbasell-chemicals-technical-literature-vapor-pressure-of-aqueous-propylene-glycol-solutions-2518.pdf)). The vapor pressure of pure glycerin at room temperature is more
126 than 100 times less, at 1.68×10^{-4} mm Hg (Pubchem
127 <https://pubchem.ncbi.nlm.nih.gov/compound/Glycerol#section=Vapor-Pressure>). Therefore we
128 expect PG to evaporate far more rapidly than VG. But the addition of as little as 10% water to a
129 pure PG compound increases the vapor pressure by a factor of 60 (Lyondell basell
130 [https://www.lyondellbasell.com/globalassets/documents/chemicals-technical-literature/
131 lyondellbasell-chemicals-technical-literature-vapor-pressure-of-aqueous-propylene-glycol-
132 solutions-2518.pdf](https://www.lyondellbasell.com/globalassets/documents/chemicals-technical-literature/lyondellbasell-chemicals-technical-literature-vapor-pressure-of-aqueous-propylene-glycol-solutions-2518.pdf)). This is relevant because most PG/VG solutions also include some water.

133
134 Wright et al., (2016) measured the evaporation kinetics of glycerin, finding that the modeled
135 times required to evaporate a 350 nm diameter glycerin particle to half its mass varied between 3
136 and 200 s depending on the amount of water vapor present. Oldham et al., (2018) studied the
137 particle distributions from 20 e-cigarette fluids sampled at the beginning, middle, and near the
138 end of the consumption of the cartridge volume. Oldham also examined the fluid composition
139 and found the sum of VG and PG to be around 80-90% of the total volume; water accounted for
140 8-16% of the remainder, with nicotine at about 2-4%. Pratte et al., (2016) also measured size
141 distributions of four e-cigarette formulations using two different methods of sampling the
142 aerosol. One method required a delay of 3.4 s compared to the second method. In this short
143 time, coagulation and evaporation/condensation processes resulted in increasing the MMAD
144 from a range of 0.18-0.20 μm to a larger range of 0.22-0.29 μm . Zhao et al., (2016) measured
145 heating coil temperatures in four e-cigarette devices and found a range from 152.3 to 216.8 $^{\circ}\text{C}$.
146 Williams et al., (2013) dissected 22 cartomizers and determined that the filaments consisted of a
147 thin nickel-chromium wire coupled to a thicker copper wire coated with silver. There were four
148 tin solder joints coupling the copper-silver wire to the air tube and mouthpiece. The aerosol
149 contained particles $>1 \mu\text{m}$ comprised of tin, silver, iron, nickel, aluminum and silicate, together
150 with nanoparticles of tin, chromium and nickel. Saffari et al., (2014) also compared particulate
151 metals from e-cigarettes and tobacco cigarettes.

152
153 Ingebretsen et al., (2012) used two methods to study e-cigarettes in an undiluted state and under
154 normal conditions of high dilution. They found an order of magnitude less mass in the latter
155 (normal) condition suggesting significant evaporation taking place on a time-scale of minutes.
156 Fuoco et al., (2014) analyzed volatility at three temperatures (37, 100, 170 C) and found the

157 particle number decreased by about half between the low and high temperatures, suggesting
158 rapid evaporation. Feng et al., (2015) applied a computational fluid dynamics model to both
159 conventional and e-cigarettes as they move through the first 3 bifurcations in a lung deposition
160 model. They found that the e-cigarette droplets, being more hygroscopic than the conventional
161 tobacco aerosol, increased in size more rapidly on encountering the humid environment of the
162 lung. Mikheev et al., (2016) applied high-time-resolution spectroscopy to characterize particle
163 size distributions of e-cigarette mainstream smoke and found a bimodal distribution between
164 nanoparticles at about 11-25 nm count median diameter (CMD) and larger particles of 96-175
165 CMD. They found the highest concentration of nanoparticles occurring in the first 0.3-0.5 s of
166 the puff. They found increased metal content in the nanoparticles that was attributed (in part) to
167 contact of the liquid with the heated coils of the atomizer. Li et al., (2020) tested e-liquids with
168 different PG/VG ratios, introducing the smoke into a 0.46 m³ chamber. Half-lives for the
169 number and mass loss rates ranged from 15-24 minutes and 6-12 minutes, respectively.

170
171 We note that studies using smoking machines are unable to measure the impact on non-vapers of
172 nearby vaping. For that, we require a human to inhale the e-cigarette aerosol into his lungs and
173 exhale it into a room. Because almost no sidestream aerosol is produced by an e-cigarette, the
174 exhaled aerosol is the only contributor to indoor concentrations and personal exposures. These
175 aerosols will undergo changes in the lungs and will mix with gases from the bloodstream to form
176 a new mixture quite different in humidity, temperature, composition, and particle size from the
177 aerosols directly created by the e-cigarette before inhalation (Martuzevicius et al., 2018). Long
178 et al., (2014) collected exhaled aerosols from human subjects and determined that the
179 distribution and mass balance of exhaled e-cigarette aerosol composition was greater than 99.9%
180 water and glycerin (about 75% water, 25% glycerin). Exposure to e-cigarette aerosol exhaled by
181 human subjects has been studied by several investigators (Baassiri et al., 2017; Logue et al.,
182 2017; Sleiman et al., 2016; Zhao et al., 2018; Schripp et al., 2013; Czogala et al., 2014; Ruprecht
183 et al., 2014, 2017; and Ballbé et al., 2014). Zhao et al., (2017) studied 13 smokers in a large
184 room and employed several monitors to measure the proximity effect. Other studies considering
185 passive vaping are available Geiss et al., 2015; Grana et al., 2014; Hess et al., 2016; Maloney et
186 al., 2016; McAuley et al., 2012; O'Connell et al., 2015). Useful studies of the “topography” of
187 vaping e-cigarettes (frequency of inhalation, amount of vapor inhaled, length of time the vapor is
188 inhaled and exhaled, etc.) have been provided (Robinson et al., 2015; Dautzenberg et al., 2015;
189 Hitchman et al., 2014; Talih et al., 2015; Public Health England, 2016).

190 191 **1.2 Marijuana liquid**

192
193 Vaping marijuana has emerged as a popular method of delivering marijuana. This method heats
194 marijuana in liquid form to the point of vaporization, avoiding combustion. The marijuana is
195 thus delivered without the accompanying products of combustion. In 2018, 6%, 14%, and 16%
196 of 16 million 8th, 10th, and 12th grade high school students, respectively, reported vaping
197 marijuana (Johnston et al., 2019). Goodwin et al., (2018) reported increases of marijuana use in
198 homes with children from 4.9% in 2002 to 6.8% in 2015. The composition of mainstream and
199 sidestream marijuana smoke, including concentrations, particle size distributions, and chemical
200 species has been studied by several investigators, almost all using machine-smoked marijuana
201 cigarettes (Hiller et al., 1984; Moir et al., 2008).

202
203 However, as with e-cigarettes, most passive exposure to vaped marijuana smoke will come from
204 the exhaled breath of smokers. In the case of vaping marijuana liquid, 100% of the passive
205 exposure will be from exhaled breath since there is no sidestream aerosol. The aerosol emerging
206 from exhaled breath will be different in many respects from the inhaled aerosol, due to lung
207 deposition, humidification, growth, and coagulation, so it is important to test exposure under
208 real-world conditions using human smokers/vapers. One recent study included 193 persons, of
209 whom about 22%, 15%, and 13% were tobacco, marijuana, and e-cigarette users, respectively
210 (Klepeis et al., 2017). The authors found that nonsmokers exposed to persons smoking either
211 tobacco or marijuana cigarettes had roughly twice the exposure to fine particles as nonexposed
212 nonsmokers. On the other hand, e-cigarettes produced no measurable increase. As part of the
213 same study, Posis et al., (2019) studied 298 homes with at least one cigarette smoker and at least
214 one child under the age of 14. In 29 homes, marijuana smoking was reported. Homes with only
215 marijuana smoking during weekly measurements using Dylos monitors had particle number
216 concentrations about 50% higher than in homes with no smoking of any kind. The Dylos
217 monitors used in both of these studies were not calibrated by comparison to gravimetric levels,
218 so the investigators could not estimate $PM_{2.5}$ exposures or source strengths. A later study has
219 found that vaping marijuana at a rate of one puff per hour for 16 hours per day can produce
220 secondhand $PM_{2.5}$ exposures comparable to those from smoking tobacco cigarettes (Wallace et
221 al., 2020). This same study found that increasing the time heating the marijuana liquid to higher
222 temperatures produced higher source emissions. A companion study determined source strengths
223 (mg/puff) for four methods of inhaling marijuana: joints, bong, glass pipes, and vaping (Ott et
224 al., 2021).

225

226 **2. Methods and Materials**

227

228 The Piezobalance is manufactured by Kanomax, Inc. Japan, and for a time was licensed for sale
229 in the US by TSI Inc, Shoreview, MN. Piezobalances used in this study included models from
230 both Kanomax USA Inc. (Andover NJ, Model 3511), and TSI, Model 8510. The instrument
231 employs a vibrating quartz crystal exposed to a steady flow rate (1 L/minute) that has passed
232 through an electrically charged $PM_{2.5}$ impactor (Sem et al., 1977). A reference crystal not
233 influenced by ambient air vibrates at a different (higher) frequency. As the exposed crystal
234 collects particles, its oscillation frequency decreases due to the piezoelectric principle, and within
235 a certain frequency range the change in frequency is proportional to the amount of material
236 collected on the exposed crystal. The proportionality depends on the crystal's properties and is
237 set by the manufacturer. The frequency change during each measured time interval is then
238 multiplied by the factory-set conversion factor G to give an estimate of the amount of mass
239 collected during the time interval (see Supplemental Information). For any given aerosol source
240 such as tobacco cigarettes, the mass usually continues to accumulate on the Piezobalance crystal,
241 and the frequency of the exposed crystal decreases proportionally due to the piezoelectric effect.
242 This causes the *difference* in frequency between the unexposed and exposed crystals to increase.
243 When the frequency difference increases beyond an upper threshold limit, the surface of the
244 crystal must be cleaned manually with a sponge and soap solution. Any decrease in the
245 frequency difference would indicate the crystal is losing mass.

246

247 The aerosol from an e-cigarette consists mostly of a liquid aerosol. As the e-cigarette's aerosol
248 accumulates on the Piezobalance crystal while it is also evaporating, the addition to the mass still
249 causes the frequency difference to increase for a while. Eventually, however, the rate of
250 evaporation exceeds the rate of accumulation, and successive one-minute Piezobalance
251 frequency differences begin to decrease instead of increasing. This turns out to be a highly
252 valuable property, since it allows a quantitative estimate to be made of the fraction of the e-
253 cigarette vapor that is volatile. When the Piezobalances used in this study were purchased, we
254 requested that a special connector be added by the seller (see details in Supplementary
255 Information). This modification allows the frequency difference between the exposed and
256 unexposed crystals to be output each minute to a computer where it can be logged, and, using the
257 monitor's conversion factor, the amount of PM_{2.5} mass accumulated or lost in units of ng/minute
258 can be computed externally and stored. A newer version of the Piezobalance includes automatic
259 datalogging for up to 500 measurements ([https://www.kanomax-usa.com/product/piezobalance-
260 dust-monitor-3520-series/](https://www.kanomax-usa.com/product/piezobalance-dust-monitor-3520-series/)). It is not clear, however, whether this newer model can log the
261 crystal's frequency or send the frequency readings to an external data logger. A design
262 modification might allow this important feature to be included in a future model.
263 The SidePak™ (TSI, Model AM510) uses a laser to sense particles as they pass through a
264 chamber. The scattered light is collected and used to estimate particle volume applying Mie
265 scattering formulae. The SidePak is calibrated using ISO 12103-1 Test Dust (formerly Arizona
266 Test Dust; specific gravity 2.6). As with all optical monitors, it is recommended that the
267 particular aerosol mixture being studied be analyzed using gravimetric methods, so that a
268 calibration factor can be determined for that aerosol. For example, the calibration factor for the
269 SidePak has been found to be about 0.32 for tobacco smoke (Dacunto et al., 2013). For the e-
270 cigarette, we have not found it possible to collect enough particles to determine a SidePak
271 calibration factor for a reason to be discussed below. Therefore, for e-cigarettes we report the
272 SidePak values exactly as recorded (calibration factor CF = 1.0). The calibration factor (CF) is
273 the ratio of the mass concentration obtained by the “gold standard” of a filter-and-laboratory-
274 microbalance to the mass concentration reported by the monitor by itself. Depending on the
275 density, humidity, and refraction and reflection index of the exhaled e-cigarette vapor, it is likely
276 that the SidePak is overestimating the actual concentration. During the study, both monitor types
277 were zeroed, the impactors were cleaned and regreased, and the flow rates were checked.

278

279 **2.1 e-cigarettes**

280

281 Two e-liquids were obtained commercially. One contained propylene glycol (PG) at 100%
282 concentration (Aphrodite's Affair, Zeusjuice, <https://www.zeusjuiceonline.com/>). The second e-
283 liquid contained glycerin or “vegetable glycerin” (VG) at 99.7% concentration (Vape Wild,
284 company out of business as of Sept 9, 2020). No nicotine was present in the two e-liquids. PG
285 is more than 100 times more volatile than VG (vapor pressure of ~0.1 mm Hg vs. 1.68 X 10⁻⁴
286 mm Hg at 25 °C).

287

288 Between May 7 and August 8, 2018, 88 experiments were carried out on the 99.7% VG e-
289 cigarette fluid in two locations. One location was a 43 m³ room in a residence in Redwood City,
290 CA. The other location was a 30 m³ room in a residence in Santa Rosa, CA. Rooms were sealed

291 off from the remainder of the home. The HVAC system in Santa Rosa was on and the floor
292 registers sealed. The HVAC system in Redwood City was off and floor registers unsealed. In the
293 Redwood City location, 54 experiments were performed using four co-located Piezobalances.
294 (In all, 6 Piezobalances were tested.) In the Santa Rosa location, 34 experiments were carried
295 out using two Piezobalances. The two locations were chosen partly in order to maximize the
296 number of different Piezobalances in case different quartz surfaces might have different effects
297 on measured volatility. Also the room sizes were quite different, with the larger room almost
298 50% larger. This would affect the time to reach good mixing, and in fact we showed that for
299 marijuana vaping, mixing was achieved in less than an hour, but for e-cigarettes even the smaller
300 room could not reach well-mixed conditions.

301

302

303 The commercial vaping device we used is designed with a tank to hold the vape liquid. This was
304 heated by an electric coil activated by pressing a button on the device, called a Reactor
305 (HaloCigs <https://www.halocigs.com/>). The power could be set by the operator and varied
306 between 10 to 50 watts. A slit could be opened to allow more or less air to mix with the heated
307 vapor. Most experiments used a fully open slit, which was found to produce the largest
308 quantities of vapor. The inhale period was shown on the Reactor's display for each inhalation,
309 and normally ranged between 2 and 3 seconds.

310

311 In all experiments, from 1 to 5 puffs were inhaled over 2-3 seconds per inhalation and exhaled
312 after holding in mouth and lungs for 1-2 seconds. The rooms were sometimes equipped with a
313 small table fan to promote mixing, but a number of experiments used no fan. Because we
314 expected that PG would evaporate far more rapidly than VG based on their vapor pressures, we
315 carried out a sequence of experiments vaping 100% PG at various distances from the
316 Piezobalance ranging from 0.3-3 m. All distances were recorded. The variation of these
317 distances is important because the rapidity of the evaporation ensures that the room has no time
318 to become well-mixed.

319

320 Room concentrations were monitored at 1-minute time intervals. Sufficient time was allotted
321 after each experiment for the room to return to the background value before another experiment
322 was attempted. This allowed the decay rates to be determined for the Piezobalance.

323

324 **2.2 Marijuana vaping**

325

326 Several commercial marijuana liquids were acquired with a range of CBD/THC ratios including
327 2:1, 8:1 and 18:1 (Care By Design, www.cbd.org). A battery and heating coil in the vaping pen
328 provided the energy to heat the attached liquid-containing cartridge. The vaping pen was
329 obtained from AbsoluteXtracts (ABX; <https://www.abx.org>). Like the Reactor for the e-
330 cigarette, the vaping pen was an electronic device that could be controlled by a button on its side.
331 Background concentrations were collected for at least 5 minutes before taking a puff of the
332 marijuana liquid. For the first 105 tests, a single protocol (Protocol I) was followed. This
333 protocol included a 2-3-second heating period (caused by pressing and holding down the power
334 button on the vaping pen), followed by a 2-3-second inhalation and an immediate exhalation.
335 The number of puffs varied from 1 ($N = 54$) to 2 ($N = 31$) to 3 ($N = 14$) to 4 ($N = 6$). Later we

336 wished to test the effect of higher temperatures on the amount of aerosol exhaled, so we adopted
337 Protocol II. Only one puff per test ($N = 19$) was employed. In this protocol, we first pressed and
338 held down the power button for 6 seconds, paused for a few seconds, and then pressed and held
339 down the power button again for 6 more seconds, keeping it pressed while inhaling for 3
340 additional seconds, and then exhaling as before. The reason for the pause midway through
341 Protocol II was to prevent the automatic shutoff of power that occurs after the button is pressed
342 for 10 consecutive seconds. Thus, Protocol II resulted in heating the liquid for about 15 seconds,
343 compared to 4-6 seconds for Protocol I.

344

345 Concentrations were measured for a number of hours after each test. Because of the slow release
346 of material from the Piezobalance crystal, some experiments lasted as long as 18-21 hours.

347

348

349

350 **2.2.1 Gravimetric tests**

351 Gravimetric tests could not be carried out on the e-cigarettes due to inability to collect enough
352 material on the filter. In contrast, gravimetric studies were possible for marijuana vaping
353 because the particles remain suspended for hours instead of minutes. Eight tests were carried out
354 at the Redwood City location using a 2:1 CBD/THC liquid, resulting in an estimated
355 Piezobalance calibration factor of $CF = 0.97$ (SD 0.03) for $PM_{2.5}$ (Zhao et al., 2020).

356

357 **2.3 Decay rates, deposition rates, and air exchange rates**

358

359 We define decay rates as the rate of total mass loss over time after a peak in mass concentration
360 occurring shortly after a source is turned off. At least three loss mechanisms are involved in this
361 decay: air exchange rates, rates of deposition on surfaces, and evaporation rates. We determined
362 air exchange rates at the Santa Rosa site by releasing carbon monoxide from cylinders containing
363 10% CO and plotting the decline of CO concentrations in the room using the Langan CO
364 Measurer Model T15, (Langan Instruments, San Francisco) capable of measuring sub-ppm
365 concentrations. A correction factor for the temperature was applied. We used SidePaks and low-
366 cost PurpleAir monitors to measure the initial $PM_{2.5}$ decay rates due to deposition and air
367 exchange combined. And we used the Piezobalance to measure the increases in decay rates due
368 to evaporation over time.

369

370 Decay rates are important to calculate for at least three reasons. 1) The length of time to return
371 to background is a crucial parameter in estimating exposure. 2) The decay rates after an initial
372 period of poor mixing can be used to estimate the source strength, another crucial parameter, in a
373 method developed by Ott (2007). 3) A change in the decay rates can indicate other processes
374 affecting aerosol loss mechanisms such as coagulation and (particularly for our purposes)
375 evaporation. For the Piezobalance, a “decay rate” is not a decline in aerosol concentration; it is a
376 rate of mass accumulation, in units such as ng/minute. Without evaporation, the rate of mass
377 accumulation is a constant multiple of the aerosol concentration. With evaporation from the
378 crystal, the rate of mass accumulation is slowed, and the decay rate (slope of the mass
379 accumulation) appears to accelerate. If the rate of mass loss from the crystal exceeds the rate of
380 mass accumulation, the mass accumulation rate becomes negative. The time integral over this

381 negative interval represents the total mass loss. This can be compared to the total mass gain
382 from the beginning of the experimental period to determine the fractional mass loss (volatility).

383

384 **2.4 Temperature and relative humidity (RH)**

385

386 At the Santa Rosa site, temperature and RH were measured every minute using Hobo Onset data
387 logger Model UX100-011. An HVAC system kept the temperature controlled to 24 (± 2) °C.
388 Although the RH was not controlled, the variation over any particular experiment was not
389 expected to be large.

390

391 **3.1 Volatility calculations**

392

393 Two equivalent methods were developed for calculating the volatile fraction of the exhaled
394 vapor (fraction lost to evaporation). Method 1 is direct observation of the frequency change over
395 time. The frequency change increases from a baseline to a peak value, and then decreases as the
396 crystal loses mass. The amount of the decrease divided by the amount of the increase over a
397 period of time following the peak is the fraction $F(t)$ of the aerosol that is lost during that time.
398 If the decay is followed long enough for the frequency to achieve an asymptotic (steady-state)
399 value, then this ratio is the total volatile fraction F_{∞} . If we have a series of measurements of the
400 observed fraction $F(t)$ ending at different times t , then we can fit an asymptotic curve of the form

401

402

$$F(t) = F_{\infty}(1 - \exp(-t/\tau))$$

403

404 to estimate the two unknown parameters F_{∞} (total fraction of material that evaporates) and time
405 constant τ (time from the beginning of the decay period to reach $1 - 1/e$ of the final concentration).
406 If different substances were tested during these experiments, the point estimates of F_{∞} and τ
407 would represent typical values for the ensemble as a whole, while the range of results would
408 reflect, in part, different possible values for the different substances tested. This formula can also
409 be used during a single experiment to estimate F_{∞} and τ for the particular vaping liquid used in
410 that experiment.

411

412 Method 2 uses the minute-by-minute direct measure of the mass gained or lost. Each positive
413 concentration value recorded by the Piezobalance following the puff is a measure of the
414 additional mass collected on the crystal. For our specific Piezobalances, the mass gain (or loss)
415 is measured in ng/minute. However, it is only the *net* additional mass, reduced by any losses
416 occurring that minute due to evaporation. After a time, the positive values change to negative
417 values. This happens when the evaporative loss exceeds the additional mass collected during
418 that minute. Since we know the Piezobalance flow rate (1 L/min), we can interpret a negative
419 value as the amount of mass (in ng) lost during that minute. Thus, we can add the consecutive
420 measured positive concentrations to obtain an estimate of the total mass collected by the
421 instrument. We can then add the negative values during the “loss time” (time when the
422 Piezobalance is reading negative values) to obtain an estimate of the total amount of mass lost
423 from the crystal due to evaporation. The absolute value of the ratio of the mass lost to the mass
424 gained over a time t measured from the beginning of the decay period is the volatile fraction $F(t)$.

425 If the period of time extends to a time when the Piezobalance is no longer recording negative
426 values, we have a direct measurement of the total fraction F_{∞} of the aerosol that is volatile.

427

428 The two methods are completely equivalent, since the frequency change over time is directly
429 related to the mass gained or lost during that time. The frequency method is convenient and
430 easier than the concentration summation method, but the latter has the advantage of being more
431 relatable to the observed concentrations.

432

433 **4.1 Results**

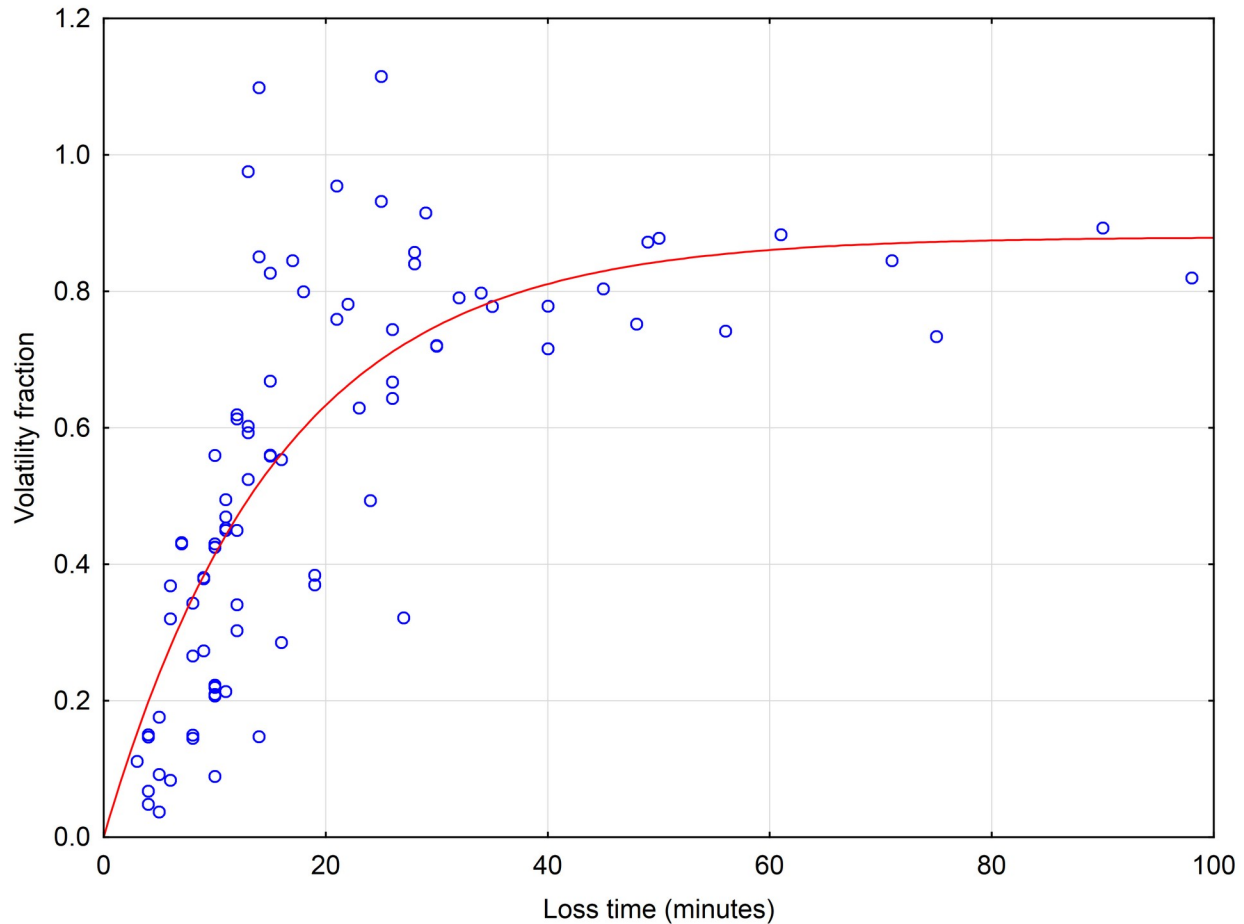
434

435 **4.1.1 e-cigarettes**

436

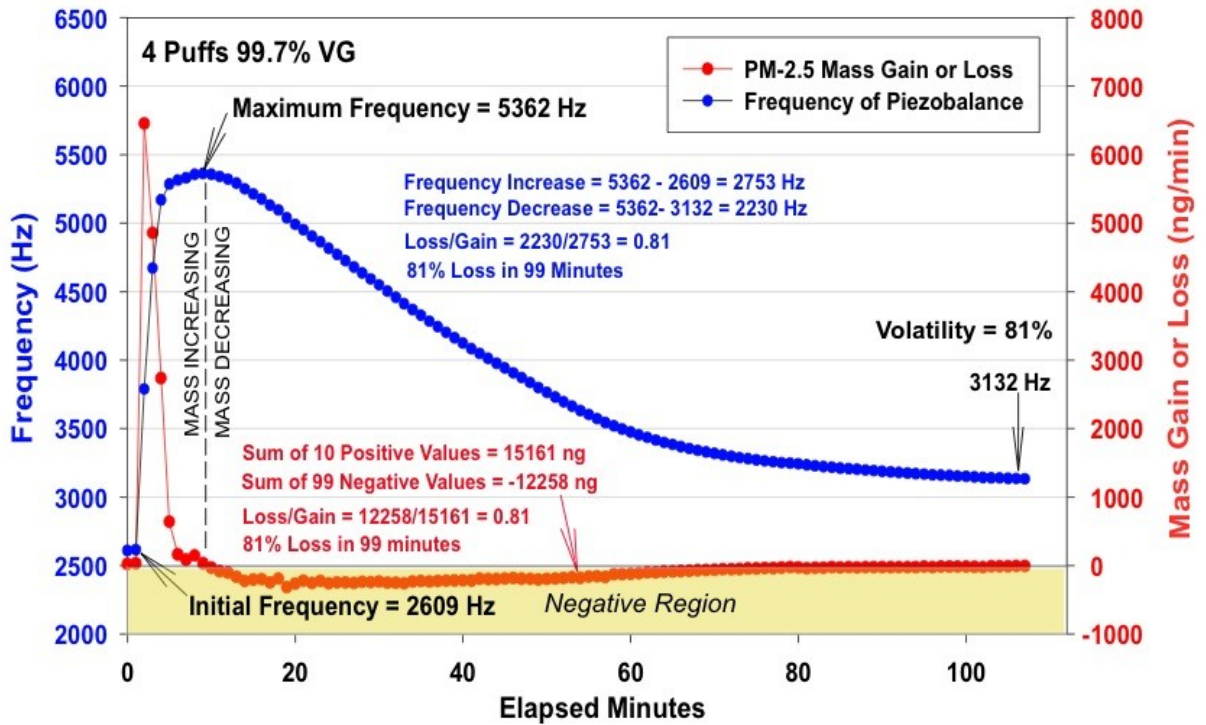
437 A total of 88 experiments on the e-liquid containing 99.7% VG were carried out comparing the
438 fraction $F(t)$ of material volatilized over a given period of time (i.e., the period we call “loss
439 time” when the Piezobalance is showing net losses of material) ranging from 3 to 99 minutes. A
440 nonlinear estimate of the asymptotic fraction F_{∞} is 0.88 (95% CI 0.77-0.99) (Figure 2). The
441 characteristic time τ was 15.7 minutes (95% CI 11.3-20.1 minutes). The time to reach 95%
442 evaporation is 3τ or 47 (CI 34-60) minutes. The estimate of 88% volatile material is in
443 reasonable agreement with the findings of Long (2014) that about 75% of the material in exhaled
444 breath following e-cigarette (VG) inhalation is water.

445



446
 447 **Figure 1. Fraction of Piezobalance particle mass evaporated over the time the**
 448 **Piezobalance is losing mass (the “loss time”). All 88 experimental results are shown. The**
 449 **dozen longest experiments all lie within the 70-90% range. The asymptotic fraction F_{∞} is**
 450 **88% (CI 77-99%), and the time to reach 95% of the total is $3\tau = 47$ minutes (CI 33-60**
 451 **minutes).**

452
 453 An experiment on 5/12/2018 illustrates the two methods of determining the volatile fraction $F(t)$
 454 for an e-cigarette (Figure 2). On this day, four puffs of an e-cigarette consisting of 99.7% VG
 455 were taken in rapid succession, and the decay was followed for 99 minutes after the peak
 456 concentration was achieved. As shown by the curve and text shown in blue on the figure, the
 457 frequency difference between the exposed and unexposed crystals increased from 2609 Hz to a
 458 peak of 5362 Hz over a 10-minute period. The frequency then declined to a new apparent steady
 459 state of 3132 Hz over the next 99 minutes (the loss time shown in Figure 1). The ratio of the
 460 frequency loss to the frequency gain was 0.81, indicating that 81% of the aerosol was volatilized
 461 after 99 minutes ($F(99) = 0.81$). This estimate agrees perfectly with the one obtained from
 462 adding up the 99 negative readings and comparing to the sum of the 10 positive readings at the
 463 beginning of the experiment, which is illustrated by the red curve and text shown on this figure.
 464 The blue curve and numbers on Figure 1 illustrate Method 1, and the red curve and numbers
 465 illustrate Method 2 of analyzing the Piezobalance decay rates. Both methods yielded the same
 466 volatility estimate of 81%.



468

469

470

471

472

473

474

475

476

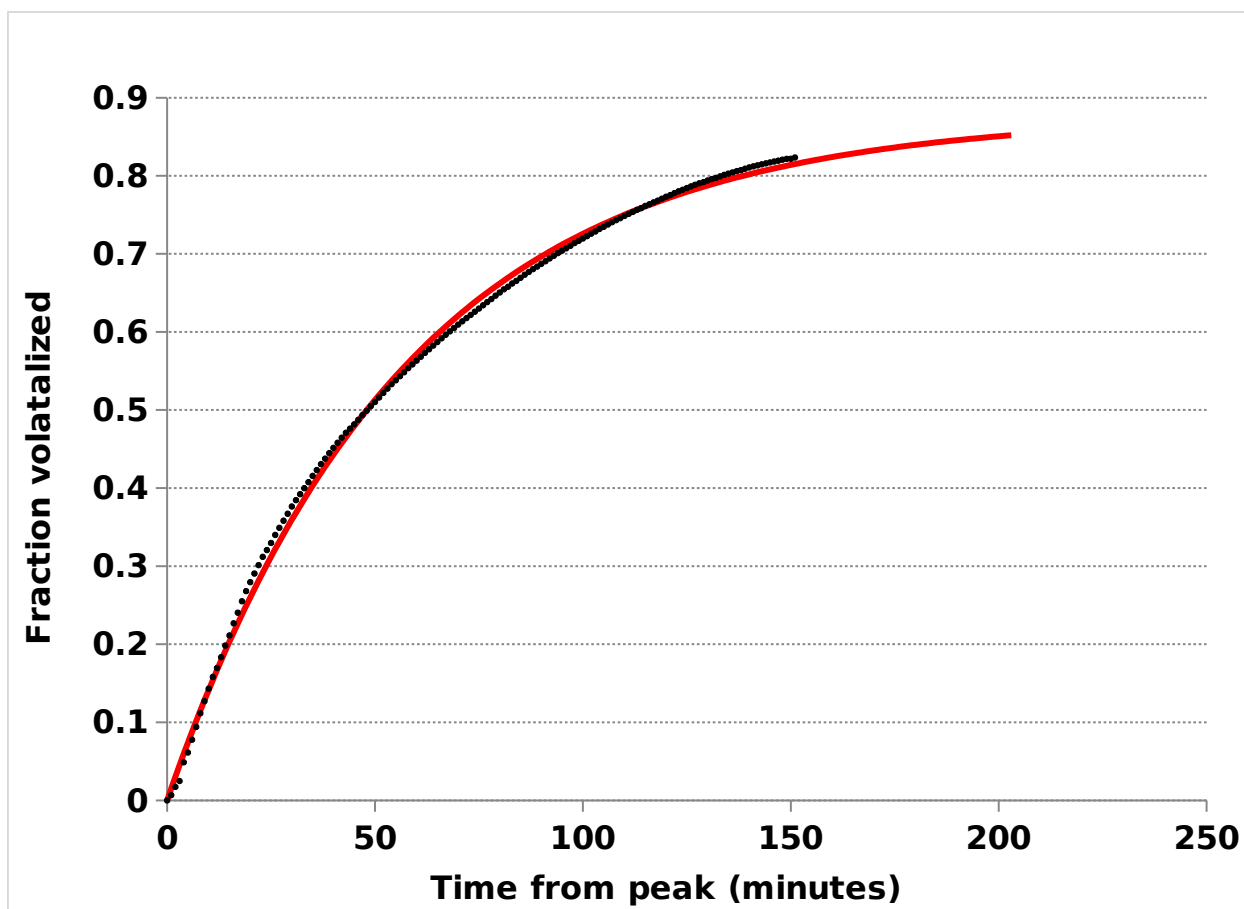
477

478

479

Figure 2. Experiment showing loss of volatile material from the e-cigarette vapor as a function of time. Change in frequency (blue) and mass accumulation (red) of the Piezobalance following 4 puffs from an e-cigarette. Methods 1 and 2 show the same volatility of 81%.

An example of a single daily experimental session at the Redwood City site comparing the mean concentrations of 99.7% VG aerosol recorded by 3 Piezobalances is provided (Figure S1). It is also possible to fit a single experimental result using the same approach. Measuring from the frequency maximum, one calculates for each time step the fraction $F(t)$ of the total frequency gain ($F_{peak} - F(0)$) that is lost during that time step. Nonlinear estimation can then be used to determine the two parameters F_{∞} and τ . An example is provided (Figure 3).



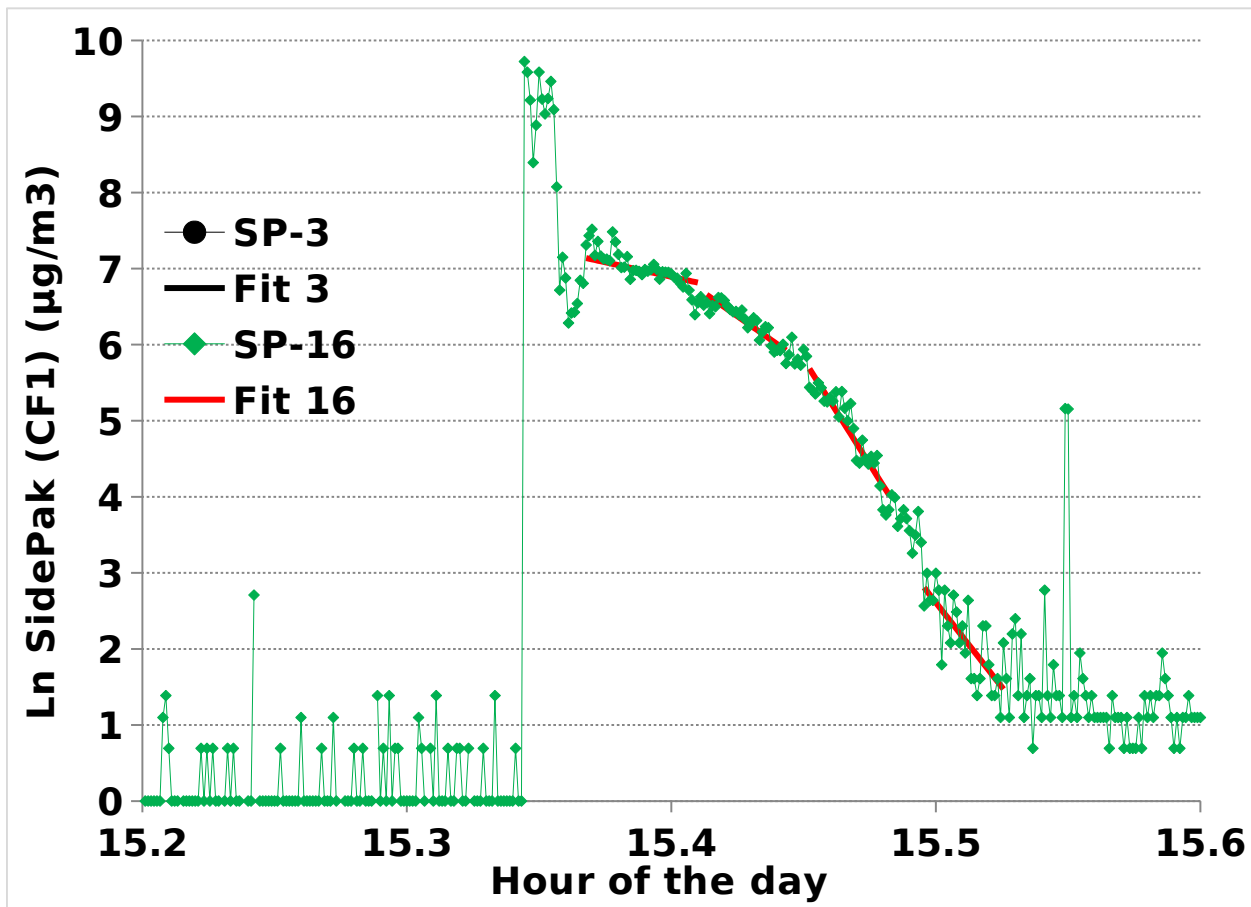
480
481
482
483
484
485

Figure 3. On 9/14/2019, the measured e-cigarette fraction volatized as a function of time $F(t)$ from a vaping fluid of 35/65 PG/VG was fit using nonlinear estimation to determine the two parameters F_{∞} and the characteristic time τ in the equation $F(t) = F_{\infty} ((1-\exp(-t/\tau))$.

486
487
488
489
490
491
492
493
494
495
496
497
498
499
500
501

Measured e-cigarette decay rates for the SidePak monitors accelerate over time (Figure 4). The decay rates for the e-cigarettes are extraordinarily large and suggest that evaporation is occurring rapidly during the short residence times of several minutes. The rates are also not constant over time. There is an initial peak followed by a sharp decay, then a rise to a lower peak. We interpret this as the passage of a plume over the monitors, followed by a period of lower concentrations, and then a return to a lower peak as the aerosol becomes better mixed. For the first 1 or 2 minutes after this secondary peak, during which the concentration may drop to 10% or even 1% of the peak, there is one decay rate that can be fitted usually with an R^2 value above 98%. Over the next period of some seconds, the decay rate increases sharply. Finally, it appears to level off at values on the order of 5% or less of the initial values. We interpret the *initial* rates as driven by evaporation, since the observed rate is on the order of 50 h^{-1} , far greater than the rates of deposition + air exchange, which are normally on the order of 0.4 h^{-1} for $\text{PM}_{2.5}$ deposition (Özkaynak et al., 1996) and range between 0.1 and 2 h^{-1} for air exchange rates (Chan et al., 2013). The subsequent *increase* in the rates is also related to evaporation, and marks a period of shrinkage of the droplets as noted by Hinds (1999). The rate of evaporation is controlled by the

502 rate at which molecules can diffuse away from the droplet. The rate increases because as the
 503 particles shrink, it is easier for molecules to escape from the more strongly curved surface (the
 504 Kelvin effect). (However, a calculation of the Kelvin effect for 0.1 and 0.4 μm droplets suggests
 505 that the Kelvin effect alone only accounts for 16% and 6% of the increase in evaporation rate,
 506 whereas our observed increases in the rate seem to be larger). Hinds (1999) includes a graph
 507 (Figure 13.11, p. 298, 2nd edition) showing a similar shape to our Figure 4 with a gradually
 508 increasing rate of shrinkage of the droplets. The graph in Hinds (1999) shows that the time for
 509 the droplet diameter to approach zero is given in milliseconds to seconds for water droplets,
 510 whereas Table 13.3 (p. 301) shows that the droplet lifetime for larger molecules such as di (2-
 511 ethyl-hexyl) phthalate with a diameter of 1 μm is 30,000 s (20 h).
 512 The *final* much slower decay occurs after evaporation is complete and represents the deposition
 513 rate of the nonvolatile portion of the aerosol added to the air exchange rate of the room with
 514 outdoor air. The overall mean residence time – the reciprocal of the decay rate – was only 1.09
 515 minutes, and the natural logarithm of the concentration decay was curved and not a straight line.
 516 The time to return to background is also extremely short (4 minutes).
 517



518
 519
 520 **Figure 4. Acceleration of aerosol decay rates attributed to evaporation of e-cigarette**
 521 **aerosol. Data from two collocated SidePaks (4-s averages). The names SP-3 and SP-16**
 522 **identify the two SidePak monitors used in this experiment.**
 523

524 The Piezobalances also show an acceleration of decay rates over time. However, what they
 525 record is the net accumulation of mass on the quartz crystal. This varies according to *two* modes
 526 of evaporation—evaporation from the aerosol droplets in the air, and evaporation of the aerosol
 527 from the crystal surface. Evaporation from the airborne aerosol results in less mass
 528 accumulation on the crystal, and evaporation from the crystal itself adds to this loss. The
 529 Piezobalances very quickly reach a point of losing mass faster than they are gaining it. In fact, a
 530 substantial portion of experiments (14 of 76, or 18%) returned only one positive value (first
 531 minute after the puff) before a run of negative values. Since the Piezobalances are recording two
 532 modes of decay and the SidePaks only one, we expect the decay rates to be higher, and the time
 533 to return to background shorter, for the Piezobalances (Table 1).

534
 535 **Table 1. Decay rates, peak concentrations, and time to return to background for the**
 536 **Piezobalances and SidePaks in multiple experiments on e-cigarette emissions.**
 537

	Decay rates Piezos (h ⁻¹)	Decay rates SidePaks (h ⁻¹)	Peak 1- min mass gains Piezos (ng)	Peak 1-min concentratio ns SidePaks (µg/m ³)	Time to return to backgroun d Piezos (minutes)	Time to return to backgroun d SidePaks (minutes)
Valid N	64	78	88	78	76	77
Mean	55.2	39.9	1560	1248	4.0	9.9
Median	52.7	31.6	281	697	3	9
Std.Dev.	34.1	25.6	3540	1405	2.7	5.1
Std.Err.	4.3	2.9	377	159	0.3	0.6

538
 539

540 All experiments described above included an e-liquid containing 99.7% VG.

541

542 Multiple experiments were also performed on pure PG. We varied the distance from the two
 543 Piezobalances and the number of puffs as important variables, and recorded the maximum
 544 concentration (or mass accumulation rate), the decay rates, and the calculated volatility fraction
 545 (Table S1). These experiments showed that at least 8-16 rapid-fire puffs directed at the
 546 Piezobalances were required to reach large mass accumulations rates >1000 ng/min (Table 2). A
 547 nonlinear analysis showed that the number of puffs was dominant over the distance variable,
 548 with significant coefficients for all three endpoints for the number of puffs and nonsignificant
 549 coefficients for all three endpoints for the distance from the Piezobalance.

550

551 **Table 2. Effect of number of puffs of 100% PG on peak concentration (mass accumulation**
 552 **rate), decay time, and volatility fraction observed for a Piezobalance.**
 553

# of pu ffs	# tes ts	Distanc e from S5 Piezo	Peak increased mass accumula	Decay time (minut es)	Volati lity fracti on
----------------------	----------------	----------------------------------	---------------------------------------	--------------------------------	--------------------------------

		(m)	tion rate (ng/minute)		
1	2	0.3	114	1	0.16
1.5	1	0.3	211	1	0.62
2	1	0.65	139	1	0.2
4	1	0.65	113	1	0.11
8	1	0.65	1307	4	0.65
12	1	1.2	445	1	0.72
16	7	0.52	2474	6.14	0.49
20	1	0.5	54	1	0.25

554
555

556
557
558
559
560
561
562
563
564
565
566
567
568
569
570
571
572

This result suggests that 100% PG liquids produce much less aerosol than VG-containing liquids and that evaporation is extraordinarily rapid for PG aerosols, as expected from the ~100-fold higher volatility for PG (Figure S2). A comparison of pure PG results from 16 puffs vs. pure VG results from one puff shows extremely high VG/PG mass ratios (Figure S3).

4.2 Marijuana

A total of 124 marijuana vaping tests were carried out between May 21, 2018 and May 28, 2019. On 122 of those tests, one or both Piezobalances provided estimates of the volatile fraction as a function of decay time (Figure S4). Experiments were varied according to the number of puffs; the heating protocol for the vape pen (Protocol I: low temperature; Protocol II: high temperature); number of fans used; and CBD/THC ratio) (Table S2).

Basic statistics for the 124 experiments are provided in Table 3.

573
574
575
576

Table 3. Basic statistics for the 124 marijuana vaping experiments with decay times for Piezobalances S5 and S6 and averaged source strength and decay rates

	N	Mean	SD	SE	Min	10th %tile	Lower quartile	Upper quartile	Median	90th %tile	Max
Decay time S5 (h)	111	4.4	3.8	0.36	0.50	1.07	1.90	5.67	2.90	10	18
Decay time S6 (h)	85	3.2	3.0	0.33	0.50	1.00	1.55	3.23	2.25	6.5	16
Source strength (mg/puff)	124	3.1	2.3	0.20	0.36	1.00	1.28	4.28	2.38	6.30	9.97
Decay rate (h ⁻¹)	124	1.6	1.0	0.09	0.33	0.52	0.84	2.12	1.31	2.89	5.03
Air exchange rate (h ⁻¹)	29	0.13	0.04	0.008	0.06	0.08	0.09	0.15	0.12	0.21	0.23
Tmin (°C)	124	23.0	2.3	0.20	16.4	19.9	21.7	24.6	23.1	25.8	28.5
Tmax (°C)	124	26.2	3.2	0.29	18.4	22.0	23.7	29.1	26.5	29.9	31.6
Delta T (°C)	124	3.1	1.6	0.15	0.24	1.1	1.8	4.3	3.1	5.0	7.6
RH min (%)	115	42.8	4.6	0.43	35.0	37.6	38.5	47.2	42.0	48.9	52.2
RH max (%)	115	47.2	4.1	0.38	40.6	42.2	43.3	50.6	46.8	53.3	55.7
Delta RH (%)	115	4.4	1.9	0.18	1.16	2.1	2.9	5.6	4.1	7.5	9.2

577
578
579
580
581
582
583
584
585
586
587
588
589
590
591
592

The measured volatility of the marijuana aerosol depended heavily on the puffing protocol (Table 4). Using the lower-temperature Protocol I, among five tested marijuana cartridges with different CBD/THC ratios (i.e., 2:1, 8:1, and 18:1), the estimates of the volatility fraction of exhaled marijuana aerosol were only 5-7% ($N = 106$) by Piezobalances. However, using the higher-temperature Protocol II ($N = 18$), mass emissions were consistently about 3 times higher than those observed using Protocol I (7.6 mg/puff compared to 2.4 mg/puff). Presumably the increased mass consists of additional compounds with higher boiling points being released. Also, Protocol II resulted in considerably higher volatility fractions compared to Protocol I. However, to observe the full loss of material from the crystal required very long (5-20 h) decay periods. This may be due to the additional compounds being slower to evaporate from the crystal.

Table 4. Volatility fraction for two Piezobalances comparing the high-temperature marijuana vaping Protocol II to the lower-temperature Protocol I.

	N	Mean	Std. Err.	25th h	Median	75th h	Max
<i>High-temperature Protocol II</i>							
Piezobalance S5	18	0.34	0.037	0.16	0.42	0.44	0.53
Piezobalance S6	8	0.25	0.047	0.19	0.25	0.34	0.46
<i>Lower-temperature Protocol I</i>							

Piezobalance S5	92	0.07	0.012	0	0	0.13	0.47
Piezobalance S6	78	0.05	0.011	0	0	0.06	0.47

593

594 Of the various parameters such as CBD/THC ratio, number of fans, air exchange rates,
595 temperature and RH, only RH showed a significant effect in a nonlinear model for the mean
596 volatility fraction (Table 8). Although RH was about 4% higher during the times when Protocol
597 II was being used (46.2 (SD 2.5)% vs. 42.2 (4.1)%), it was not significantly higher as shown by
598 the boxplots in Figure S5. Nonetheless, the higher RH had a small but significant effect in
599 lowering the volatility fraction by about 2.5%. This presumably would be due to the higher
600 atmospheric vapor pressure reducing the aerosol evaporation rate.

601

602 **Table 5. Effect of ancillary parameters on volatility fraction**

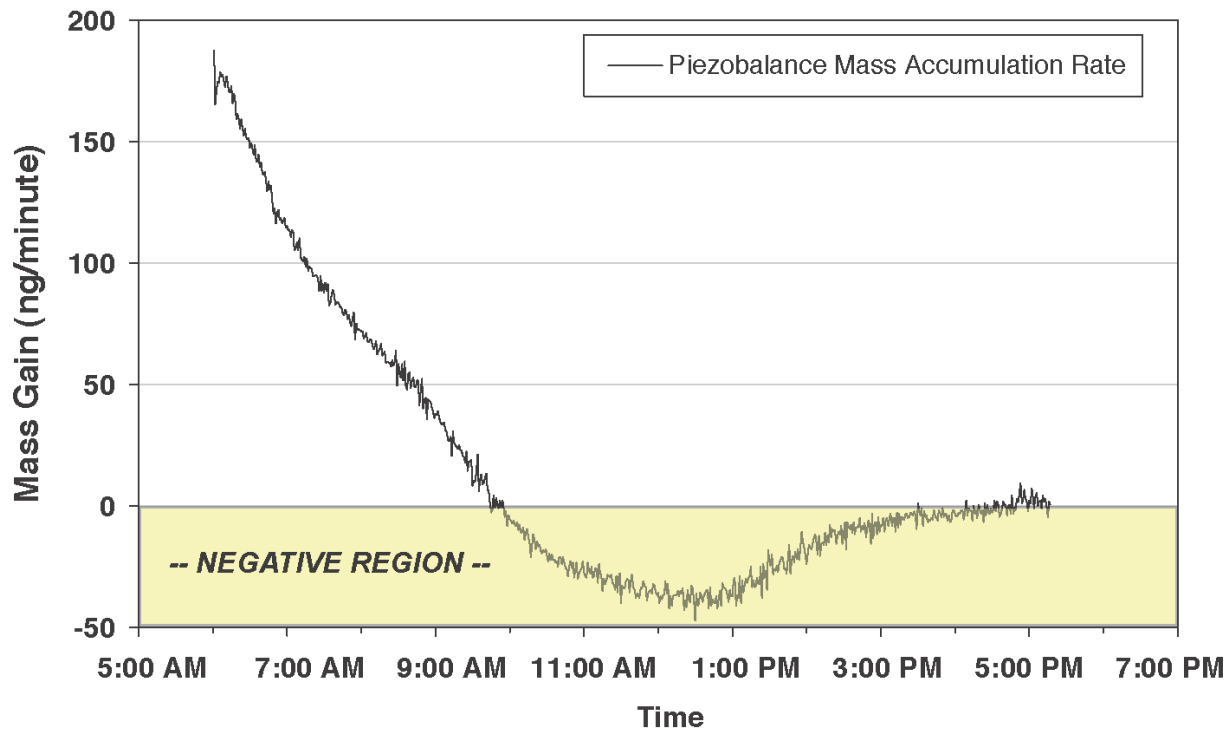
603

	Estimate	Standard error	t-value	p-value	Lower Conf	Upper Conf
protocol	0.231	0.076	3.0	0.008	0.070	0.391
RH	-0.025	0.010	-2.5	0.023	0.046	0.004
No. of puffs	0.509	0.921	0.6	0.6	-1.43	2.45
decay time	-0.003	0.007	-0.5	0.7	-0.02	0.01
decay rate	-0.195	0.126	-1.5	0.1	-0.46	0.07
Air exchange rate	-0.318	0.448	-0.7	0.5	-1.26	0.63
Temperature	0.009	0.009	1.1	0.3	-0.01	0.03
CBD/THC ratio	323.2	75748	0.0004	0.999	-1597	1598

604

605 The volatile fraction for these marijuana experiments was estimated in the same way as shown
606 above for the e-cigarette experiments. That is, the mass accumulation rates were determined
607 minute by minute, and the associated frequency curves showing the total accumulation were
608 plotted. An example is provided in Figures 5 and 6.

609



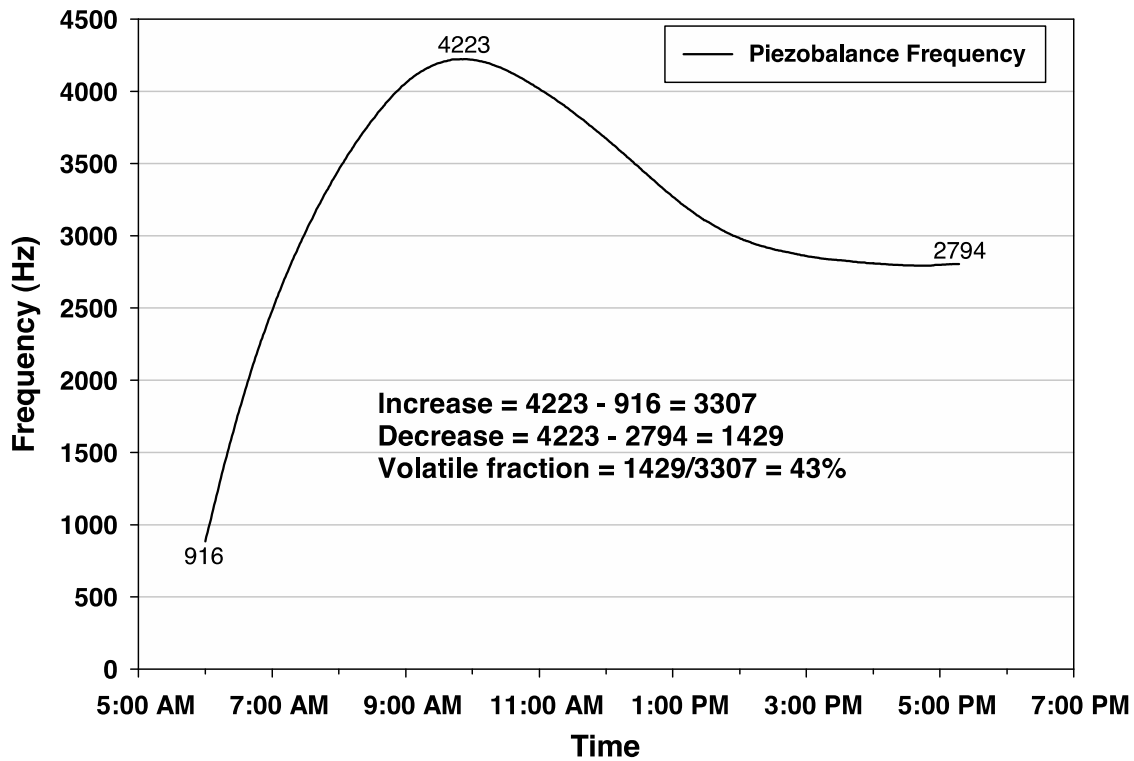
610
611

612 **Figure 5. Piezobalance mass accumulation rate in marijuana vaping experiment. On April**
613 **28, 2019, the Piezobalance showed a maximum rate of mass accumulation of about 175 ng/**
614 **minute, followed by a decline until the mass begins to be lost from the crystal, reaching a**
615 **peak loss rate of nearly 50 ng/minute before gradually returning to equilibrium about 12**
616 **hours later.**

617

618 Using Method 2 that was illustrated in Figure 2, the volatile fraction for vaping marijuana can be
619 determined directly from Figure 5 by integrating the positive and negative areas under the curve
620 and taking the absolute value of the ratio, which turned out to be 0.43. As before, Method 1
621 offers an easier way to calculate the volatile fraction directly from the frequency curve (Figure
622 6). The ratio of the decrease in frequency to its increase provides the volatility fraction.

623



624
 625 **Figure 6. Frequency curve for the same mass concentrations that were shown in Figure 5.**
 626 **Using Method 1, the volatility fraction can be determined directly from the Piezobalance**
 627 **frequency curve in this figure. The increase to the peak frequency and the decrease to the**
 628 **final equilibrium frequency provide the two values needed to determine the volatile**
 629 **fraction of 43%.**

630

631 Beginning on April 25, 2019, an 8-day series of experiments was carried out under Protocol II
632 with a single puff of 2:1 CBD/THC marijuana liquid each day. Six of the 8 experiments were
633 followed sufficiently long (8-18 hours) to determine the final volatility fraction, which averaged
634 close to 47% (SD 5%) (Table S3). This mean volatility fraction of 47% associated with Protocol
635 II is significantly ($p < 0.0001$) greater than the 5-7% values shown under Protocol I. Other
636 experiments at the Redwood City location using Protocol II also found higher source strengths
637 and volatility fractions compared to experiments using Protocol I.

638

639 Measured decay rates for both the SidePak and Piezobalance tend to accelerate over time (Figure
640 7). As a practical matter, we find that the decay rates for most experiments on marijuana vaping
641 remain constant over time for the first hour or two (usually with R^2 values $>95\%$) and then
642 accelerate. Therefore, in referring to “decay rates” it is these relatively constant *initial* rates that
643 are meant. Decay rates observed for marijuana aerosols are far lower than those for e-cigarettes,
644 reflecting the much lower volatility fraction for the marijuana aerosols. These vaping decay rates
645 are strongly affected by the use of table fans (Table 9).

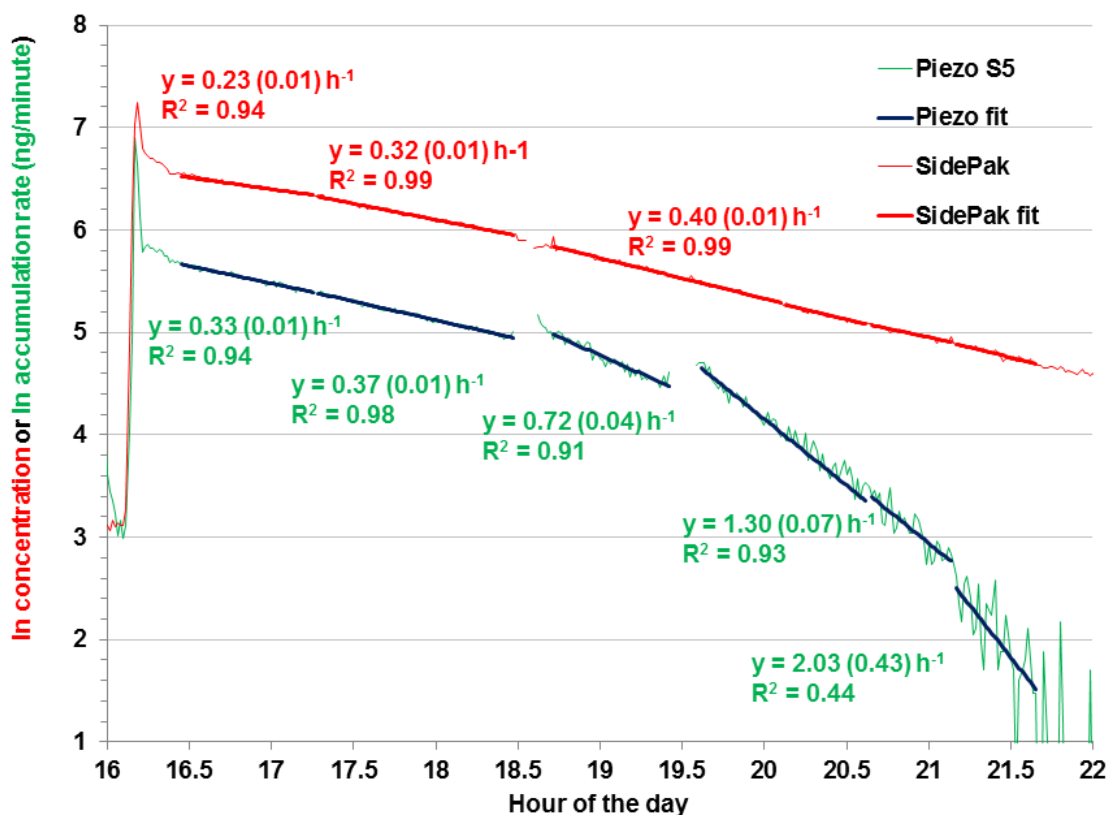
646

647 **Table 6. Piezobalance decay rates (h^{-1}) as a function of fan configuration.**

<i>Piezo decay rate</i> (h^{-1})	N	Mea n	Std.Er r.	25t h	Media n	75t h	Maximu m
fan off	8	1.22	0.07	0.7 1	1.06	1.6 5	4.27
1 fan on	2 9	2.29	0.21	1.3 4	2.10	3.1 1	5.03
2 fans on	8	3.05	0.35	2.3 9	3.04	3.8 4	4.40

648

649



650
651

652 **Figure 7. Acceleration of marijuana vapor decay rates due to evaporation. Increased rates**
 653 **measured by SidePak (red) suggest some volatility shown by the airborne aerosol.**
 654 **Increased rates measured by Piezobalance show rapid evaporation from the quartz crystal.**

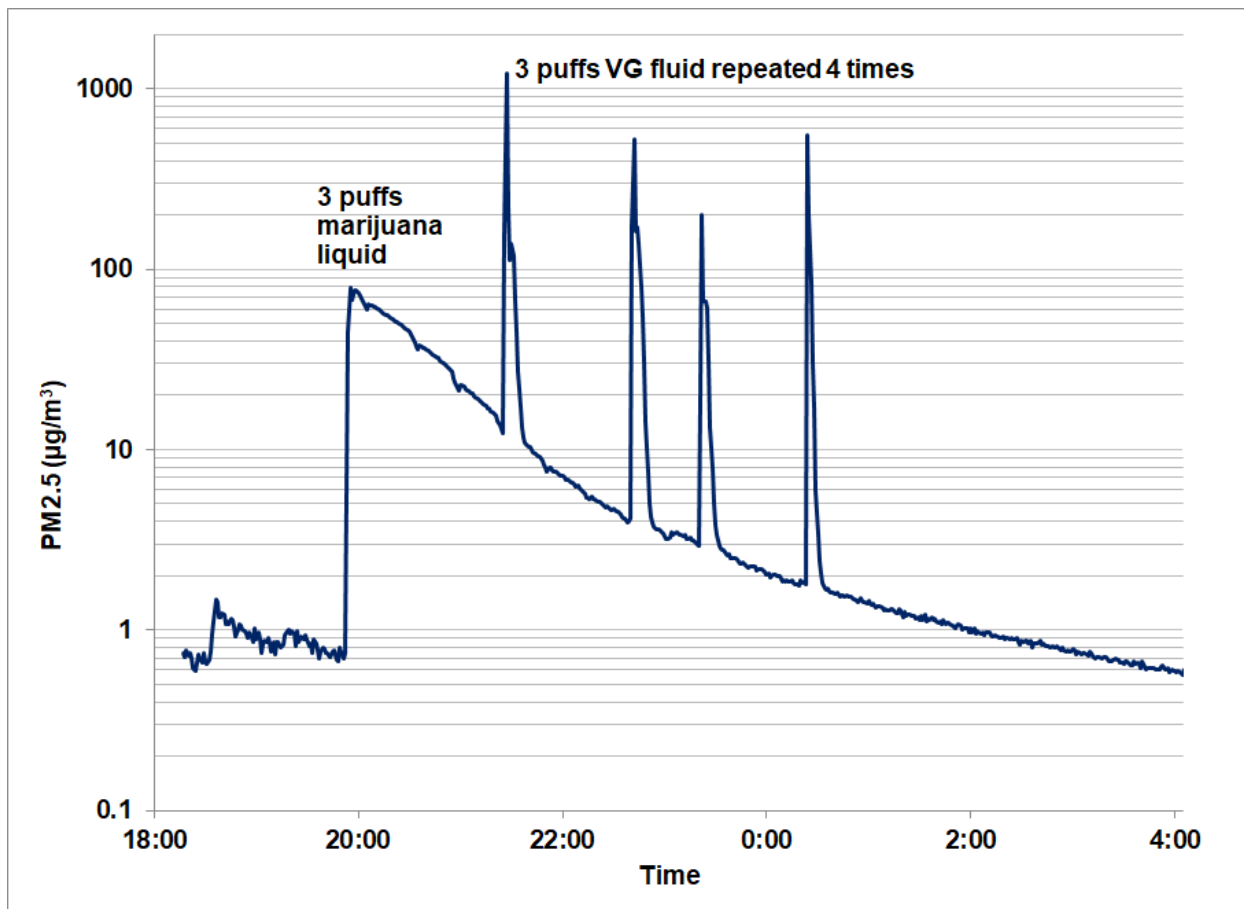
655
656
657

658 4.3 Comparison of e-cigarettes and marijuana exposures

659

660 We have found that both e-cigarettes and marijuana vaping produce aerosols showing strong
 661 concentration peaks accompanied by some volatility. However, the differences in resulting
 662 exposures are large on a per-puff basis. Figure 8 shows that the peak concentrations observed
 663 from e-cigarettes disappear in minutes, whereas the exposure from marijuana vaping can last for
 664 up to 8 hours. Secondhand exposures (concentration × time) in this example were 152 μg/m³-h
 665 for the marijuana aerosol (3 puffs) and 77 μg/m³-h for the e-cigarettes (12 puffs), or about a
 666 factor of 8 on a per-puff basis.

667
668



669
670

671 **Figure 8. Time to return to room background for e-cigarette aerosol compared to**
672 **marijuana aerosol. Following 3 puffs of marijuana liquid, on four separate occasions there**
673 **was an additional set of 3 puffs of a 99.7% pure VG e-liquid. A single instrument (the**
674 **SidePak) recorded the concentration.**

675

676 4.4 Limitations of the Study

677

678 Because the e-cigarette aerosol evaporates so rapidly, the normal approach of collecting material
679 and weighing it in a collocated gravimetric device cannot be used. We have therefore not been
680 able to determine the density of the e-cigarette aerosol, and therefore the readings of the
681 Piezobalance are only within some unknown calibration factor of the actual concentration. The
682 Piezobalance is factory calibrated using welding particles, and the density of these is not known.
683 However, multiple studies have indicated that the Piezobalance is a good estimator (within
684 $\pm 15\%$) of tobacco smoke particle concentrations (Repace and Lowrey. 1980; Ott et al., 1996).
685 For example, Fairchild et al., (1980) compared two Piezobalances to gravimetric measurements
686 of 8 aerosol sources, including coal dust, silica dust, arc-welding fumes, polydisperse phthalate,
687 etc. High R^2 values of 83-93% were obtained for 1-minute, 15-minute, 1-hour and daily samples,
688 although positive biases were observed. Earlier Sem et al., (1977) compared the Piezobalance to
689 gravimetric measures of several aerosols and found agreement within 10% for all tested aerosols
690 except for environmental tobacco smoke (15%). Ingebrigtsen et al., (1988) found general

691 agreement between the Piezobalance and gravimetric measurements of ETS, provided careful
692 flow checks were made to adjust the calibration of individual instruments.

693

694 Our study of e-cigarettes is also limited to estimating room concentrations produced by a single
695 person. With the high observed rate of evaporation, it is not possible for a single vaper to bring
696 the room air to a stable well-mixed concentration; however, for multiple vapers in one room, it
697 might be possible to attain a well-mixed condition, and in that case, there might be a slower rate
698 of decay when the vaping ceases. This case of multiple vapers may be of interest for future
699 research.

700

701 **5.1 Discussion**

702

703 Our study employed optical monitors to detect aerosol volatility, as measured by the increase in
704 the decay rate over time. We also used the Piezobalance to measure the combined losses due to
705 aerosol volatility and evaporation from the crystal surface. To our knowledge, this is the first
706 study to present a method for using the Piezobalance to estimate the volatility of an aerosol
707 mixture.

708

709 A primary finding of this investigation is the extreme rapidity with which the e-cigarette aerosols
710 return to background, ranging between just 1-10 minutes. A second finding is the large fraction
711 of the pure (99.7%) VG aerosol that is subject to evaporation, averaging 88%.

712 These two findings indicate that e-cigarette exposures will be brief following a puff and will
713 quickly fall to the background concentration. The experimental rooms were quite small, the air
714 exchange rates were very low ($< 0.4 \text{ h}^{-1}$), and therefore the concentrations measured here are
715 likely to be near the maximum concentrations observed in most homes. An average-size home
716 will be 5-10 times the volume of these rooms and thus house-wide exposures will be 5-10 times
717 lower than the values reported here. The rapidity with which the aerosol disappears will ensure
718 that good mixing will not occur throughout the home, meaning that persons a few meters away
719 from the vaper will be exposed to aerosol concentrations for a very short time. For 100% PG, the
720 aerosol concentrations will be negligible for persons at a distance $>0.65 \text{ m}$.

721

722 These findings for e-cigarettes are very different from the results reported here for marijuana
723 vaping. Exhaled marijuana aerosols remain elevated in the home for hours as opposed to about
724 6-8 minutes. Secondhand exposure to marijuana aerosol was both substantial and long-lasting,
725 with mean $\text{PM}_{2.5}$ concentrations during the nine hours after one or several puffs about 10 times
726 the background level. For most tests using Protocol I (Low to moderate temperatures), volatility
727 was low at around 5-7%. However, for Protocol II (higher temperatures), the volatility was
728 much higher at 36-45%. Because of the long residence times and relatively high $\text{PM}_{2.5}$
729 concentrations caused by marijuana vaping, future research should include studies of air
730 pollution from marijuana vaping indoors.

731

732 **6.1 Conclusions**

733

734 This paper shows that a monitor designed to measure and record mass accumulation on a minute-
735 by-minute basis can be used to estimate the volatility of the aerosols produced by vaping. For e-

736 cigarettes, a major portion (88%; CI 77-99%) evaporates within a few minutes. For marijuana
737 liquids, the major portion lasts for hours. Volatility of the marijuana liquids appears to depend on
738 peak temperature liquid reached during the heating process; low temperatures (Protocol I)
739 showed low (5-7%) volatility and high temperatures (Protocol II) showed higher (25-34%)
740 volatility. This new methodology for measuring the rate of change of the mass collected on a
741 surface on a minute-by-minute basis could enhance our understanding of aerosol dynamics
742 including volatility.

743

744 **7.1 Conflicts of interest**

745

746 The authors declare no conflicts of interest.

747

748 **8.1 Funding Source**

749 This study was supported in part by a grant awarded to Stanford University to study secondhand
750 exposure to marijuana: Agreement #28IR-0062 sponsored by the University of California Office
751 of the President; Tobacco Related-Disease Research Program (TRDRP).

752

753 **8.1.1 Ethical considerations**

754

755 As part of that grant, the Stanford Institutional Review Board (IRB) gave approval to the authors
756 to carry out human experimentation. Since no human subjects were recruited for the experiments
757 presented in this paper, telephone contact was made with a member of the IRB to obtain his
758 opinion on whether IRB coverage of the authors was needed by the IRB. His advice was that
759 IRB review is not required if the researchers doing the study are the only human subjects.

760 Finally, the emissions of every experiment were produced by a subset of the authors, who were
761 experienced in inhaling both nicotine and marijuana smoke, and no persons were present in the
762 room during the air pollutant decay periods. No other individuals participated in the smoking or
763 vaping activities, nor were any persons other than the authors exposed to the aerosols produced.

764

765 **8.1.2 Role of funding source**

766

767 The funding source had no involvement in the study design, collection, analysis, or interpretation
768 of data, writing or editing of the report, or the decision to seek publication.

769

770 **9.1 CRediT authorship contribution statement**

771

772 **Lance Wallace:** Conceptualization, Methodology, Investigation, Formal analysis, Writing -
773 original draft. **Wayne Ott:** Methodology, Software, Validation, Investigation, Formal analysis,
774 Writing - review & editing. **Tongke Zhao:** Methodology, Validation, Investigation, Formal
775 analysis, Writing - review & editing. **Kai-Chung Cheng:** Methodology, Validation,
776 Investigation, Formal analysis, Writing - review & editing, Project administration. **Lynn**
777 **Hildemann:** Writing - review & editing, Supervision, Project administration, Funding
778 acquisition.

779

780 **10.1 References**

781

782 AbsoluteXtracts. <https://www.abx.org/> (Accessed 2/28/2021)

783

784 Baassiri, M., S. Talih, R. Salman, N. Karaoghlanian, R. Saleh, R. Hage, Saliba, and A. Shihadeh.
785 2017. Clouds and “throat hit”: Effects of liquid composition on nicotine emissions and physical
786 characteristics of electronic cigarette aerosols. *Aerosol Science and Technology* 51(11):1231-
787 1239. <https://doi.org/10.1080/02786826.2017.1341040>

788

789 Ballbè, M, J. M. Martínez-Sánchez, X. Sureda, M. Fu, R. Pérez-Ortuño, J. A. Pascual, E. Saltó,
790 and E. Fernandez. 2014. Cigarettes vs. e-cigarettes: passive exposure at home measured by
791 means of airborne marker and biomarkers. *Environmental Research* 135:76–80.

792

793 Bertholon, J-F, M. H. Becquemin, M. Roy, D. Ledur, A. I. Maesano, and B. Dautzenberg. 2013.
794 Comparison of the aerosol produced by electronic cigarettes with conventional cigarettes and the
795 shisha. *Revue des Maladies Respiratoires* 30:752–757.

796

797 Care By Design, <https://www.cbd.org/> (Accessed 2/28/2021)

798

799 Chan, W., Joh, J., Sherman, M.H. Analysis of air leakage measurements of US houses
800 *Energy and Buildings* 66 (2013) 616–625

801

802 Czogala, J., M. L. Goniewicz, B. Fidelus, W. Zielinska-Danch, M. J. Travers, and A. Sobczak.
803 2014. Secondhand exposure to vapors from electronic cigarettes. *Nicotine & Tobacco Research*.
804 16:655–662.

805

806 Dacunto, P.J., K-C. Cheng, V. Acevedo-Bolton, R-T. Jiang, N. E. Klepeis, J. L. Repace, W.R.
807 Ott, and L. M. Hildemann. 2013. Real-time particle monitor calibration factors and PM_{2.5}
808 emission factors for multiple indoor sources. *Environmental Science: Processes and Impacts*, 15:
809 1511-1519.

810

811 Dautzenberg, B. and D. Bricard. 2015. Real-time characterization of e-cigarettes use: the 1
812 million puffs study. *J Addiction Research Therapy* 6:229. doi:10.4172/2155-6105.1000229.
813 <http://dx.doi.org/10.4172/2155-6105.1000229> (Accessed 2/28/2021)

814

815 Fairchild CI, Tillery MI, Ettinger HJ. *An evaluation of fast response aerosol mass monitors*.
816 Los Alamos Scientific Laboratory. LA 8220. Univ. California. UC-41. 1980.

817

818 Feng Y., Kleinstreuer C., Rostami, A. Evaporation and condensation of multicomponent
819 electronic cigarette droplets and conventional cigarette smoke particles in an idealized G3–G6
820 triple bifurcating unit. *Journal of Aerosol Science* 80 (2015) 58–74.

821

822 Fernández, E., M. Ballbè, X. Sureda, M. Fu, E. Saltó, and J. M. Martínez-Sánchez. 2015.
823 Particulate matter from electronic cigarettes and conventional cigarettes: a systematic review and
824 observational study. *Current Environmental Health Reports* 2:423–429.
825

826 Fuoco FC, Buonanno G, Stabile L, Vigo P. Influential parameters on particle
827 concentration and size distribution in the mainstream of e-cigarettes.
828 *Environmental Pollution* 2014;184:523–529. doi:10.1016/j.envpol.2013.10.010.
829

830 Geiss O., I. Bianchi, F. Barahona, and J. Barrero-Moreno. 2015. Characterisation of mainstream
831 and passive vapours emitted by selected electronic cigarettes. *International Journal of Hygiene
832 and Environmental Health* 218:169–180.
833

834 Goodwin RD, Cheslack-Postava K, Santoscoy S, et al. Trends in cannabis and cigarette use
835 among parents with children at home: 2002 to 2015. *Pediatrics*. 2018;141(6):e20173506
836

837 Grana, R., N. Benowitz, and S. A. Glantz. 2014. E-cigarettes: A scientific review (*Circulation*
838 129:1972-1986.
839

840 Halo Cigs. <https://www.halocigs.com/> (Accessed 2/28/2021
841

842 Hess I, K. Lachireddy, and A. Capon. 2016. A systematic review of the health risks from passive
843 exposure to electronic cigarette vapour. *Public Health Research & Practice* 26(2):e2621617.
844

845 Hiller, F.C., F.J. Wilson, Jr., M.K. Mazumder, J.D. Wilson, and R.C. Bone. 1984. Concentration
846 and particle size distribution in smoke from marijuana cigarettes with different Δ^9 -
847 Tetrahydrocannabinol content. *Fundamental and Applied Toxicology* 4:451-454.
848

849 Hinds, W.C. *Aerosol Technology*, 2nd edition. 1999. Wiley, New York.
850

851 Hitchman S. C., L. S. Brose, J. Brown, D. Robson, and A. McNeill. 2015. Associations between
852 e-cigarette type, frequency of use, and quitting smoking: findings from a longitudinal online
853 panel survey in Great Britain. *Nicotine & Tobacco Research* 17(10):1187–1194.
854

855 Hodas, N., Lunden, M., Meng, Q. Y., Baxter, L., Özkaynak, H., Burke, J., Rich, D., Ohman-
856 Strickland, P., Turpin, B. J. (2012). Heterogeneity in the fraction of ambient PM_{2.5} found
857 indoors contributes exposure error and may contribute to spatial and temporal differences in
858 reported PM_{2.5} health effect estimates. *J Exposure Science and Environmental
859 Epidemiology* 22: 448-454.
860

861 Ingebrethsen BJ, Heavner DL, Angel AI, Conner JM, Steichen TJ, Green CR (1988) A
862 Comparative Study of Environmental Tobacco Smoke Particulate Mass Measurements in an
863 Environmental Chamber, *J Air Pollution Control Association* 1988;38:413-417.
864 doi:10.1080/08940630.1988.10466391.
865

866 Ingebrethsen BJ, Cole SK, Alderman SL. Electronic cigarette aerosol particle

867 size distribution measurements. *Inhalation Toxicology* 2012;24(14):976–984.
868 doi:10.3109/08958378.2012.744781.
869
870 Johnston, L. D., Miech, R. A., O’Malley, P. M., Bachman, J. G., Schulenberg, J. E., & Patrick,
871 M. E. (2019). *Monitoring the Future national survey results on drug use 1975-2018: Overview,*
872 *key findings on adolescent drug use.* Ann Arbor: Institute for Social Research, University of
873 Michigan. Table 5, pp. 66-67.
874
875 Klepeis, N.E., J. Bellettiere, S. C. Hughes, B. Nguyen, V. Berardi , S. Liles, et al. 2017. Fine
876 particles in homes of predominantly low-income families with children and smokers: Key
877 physical and behavioral determinants to inform indoor-air-quality interventions. *PLoS ONE*
878 12(5): e0177718. <https://doi.org/10.1371/journal.pone.0177718> (Accessed 2/28/2021
879
880 Langan Instruments. <http://www.langan.biz/> (Accessed 2/28/2021
881
882 Levy, D. T., R. Borland, E. N. Lindblom, M. L. Goniewicz, R. Meza, T. R. Holford, Z. Yuan, Y.
883 Luo, R. J. O’Connor, R. Niaura, and D. B Abrams. 2018. Potential deaths averted in USA by
884 replacing cigarettes with e-cigarettes. *Tobacco Control* 27:18–25.
885
886 Li, L., Lee, E.S. Nguyen, C., Zhu. Y. Effects of propylene glycol, vegetable glycerin, and
887 nicotine on emissions and dynamics of electronic cigarette aerosols. *Aerosol Science and*
888 *Technology*, DOI: 10.1080/02786826.2020.1771270
889
890 Mikheev, V.B., Brinkman, M.C. Granville, C.A., Gordon, S.M., Clark P.I. Real-time
891 measurement of electronic cigarette aerosol size distribution and metals content analysis.
892 *Nicotine & Tobacco Research*, 2016, 1895–1902. doi:10.1093/ntr/ntw128
893
894 Logue, J. M., M. Sleiman, V. N. Montesinos, M. L. Russell, M. I. Litter, N. L. Benowitz, L. A.
895 Gundel, and H. Destailats. 2017. Emissions from electronic cigarettes: assessing vapers’ intake
896 of toxic compounds, secondhand exposures, and the associated health impacts. *Environmental*
897 *Science and Technology* 51:9271–9279.
898
899 Long, G. A. 2014. Comparison of select analytes in exhaled aerosol from e-cigarettes with
900 exhaled smoke from a conventional cigarette and exhaled breath. *International Journal of*
901 *Environmental Research and Public Health*. 11:11177-11191. doi:10.3390/ijerph11111177.
902
903 Lunden, M. M., K. L. Rezvan, M. L. Fischer, Thatcher, T. L., D. Littlejohn, S. V. Hering, and N. J.
904 Brown, 2003. The transformation of outdoor ammonium nitrate aerosols in the indoor environment.
905 *Atmospheric Environment* 37:5633-5644.
906
907 Lyondellbasell. [https://www.lyondellbasell.com/globalassets/documents/chemicals-technical-](https://www.lyondellbasell.com/globalassets/documents/chemicals-technical-literature/lyondellbasell-chemicals-technical-literature-vapor-pressure-of-aqueous-propylene-glycol-solutions-2518.pdf)
908 [literature/lyondellbasell-chemicals-technical-literature-vapor-pressure-of-aqueous-propylene-](https://www.lyondellbasell.com/globalassets/documents/chemicals-technical-literature/lyondellbasell-chemicals-technical-literature-vapor-pressure-of-aqueous-propylene-glycol-solutions-2518.pdf)
909 [glycol-solutions-2518.pdf](https://www.lyondellbasell.com/globalassets/documents/chemicals-technical-literature/lyondellbasell-chemicals-technical-literature-vapor-pressure-of-aqueous-propylene-glycol-solutions-2518.pdf) Accessed 2/21/21.
910

911 Maimone, F., B. J. Turpin, P. Solomon, Q.Y. Meng, A.L. Robinson, R. Subramanian and A.
912 Polidori (2011). Correction methods for organic carbon artifacts when using quartz-fiber filters in
913 large particulate matter monitoring networks: The regression method and other options, *Journal*
914 *of the Air & Waste Management Association*, 61:696-710, DOI: 10.3155/1047-3289.61.6.696.
915

916 Maloney, J. C., M. K. Thompson, M. J. Oldham, C. L. Stiff, P. D. Lilly, G. J. Patskan, K. H.
917 Shafer, and M. A. Sarkar. 2016. Insights from two industrial hygiene pilot e-cigarette passive
918 vaping studies. *Journal of Occupational and Environmental Hygiene*, 13(4):275-283. DOI:
919 10.1080/15459624.2015.1116693.
920

921 Martuzevicius, D., T. Prasauskas, A. Setyan, G. O'Connell, X. Cahours, R. Julien, and S. Colard.
922 2018. Characterization of the spatial and temporal dispersion differences between exhaled e-
923 cigarette mist and cigarette smoke. *Nicotine & Tobacco Research* 2018:1-7.
924 doi:10.1093/ntr/nty121.
925

926 McAuley, T.R., P. K. Hopke, J. Zhao, and S. Babaian. 2012. Comparison of the effects of e-
927 cigarette vapor and cigarette smoke on indoor air quality. *Inhalation Toxicology* 24(12):850-857.
928 DOI:10.3109/08958378.2012.724728.
929

930 McNeill A., L. S. Brose, R. Calder, L. Bauld, and D. Robson. 2018. *Evidence review of e-*
931 *cigarettes and heated tobacco products. A report commissioned by Public Health England.*
932 London: Public Health England.
933

934 Moir, D., W.S. Rickert, G. Levasseur, Y. Larose, R. Martens, P. White, and S. Desjardins. 2008.
935 A comparison of mainstream and sidestream marijuana and tobacco cigarette smoke produced
936 under two machine smoking conditions. *Chemical Research in Toxicology* 21:494-502.
937

938 O'Connell, G., S. Colard, X. Cahours and J. D. Pritchard. 2015. An assessment of indoor air
939 quality before, during and after unrestricted use of e-cigarettes in a small room. *International*
940 *Journal of Environmental Research Public Health* 12:4889-4907. doi:10.3390/ijerph120504889.
941

942 Oldham MJ, Zhang J, Rusyniak MJ, Kane DB, Gardner WP. Particle size distribution of selected
943 electronic nicotine delivery system products. *Food Chemistry & Toxicology* 2018;113:236-240
944

945 Ott, W.R. 2007. "Mathematical Modeling of Indoor Air Quality," Chapter 18, pp. 411-444 in
946 Ott, W.R., Steinemann, A.C., and Wallace, L.A. editors, *Exposure Analysis*, Taylor and Francis,
947 Boca Raton, FL.
948

949 Ott, W.R., Switzer, P., and Robinson, J. 1996. Particle concentrations inside a tavern before and
950 after prohibition of smoking: Evaluating the performance of an indoor air quality model *Journal*
951 *of the Air and Waste Management Association*. 46: 1120-1134.
952

953 Ott, W.R., Zhao, T., Cheng, K-C, Wallace, L.A., and Hildemann, L.M. 2021. Measuring indoor
954 fine particle concentrations, emission rates, and decay rates from cannabis use in a
955 residence, *Atmospheric Environment X*, in press.

956
957 Özkaynak, H., Xue, J., Spengler, J.D., Wallace, L.A., Pellizzari, E.D. and Jenkins, P. Personal
958 Exposure to Airborne Particles and Metals: Results from the Particle TEAM Study in Riverside,
959 CA. *J. Exposure Analysis and Environmental Epidemiology* 6:57-78, 1996.
960
961 Pankow JF. Calculating compound dependent gas-droplet distributions in aerosols of propylene
962 glycol and glycerol from electronic cigarettes. *J Aerosol Science* 2017;107: 9–13.
963 doi:10.1016/j.jaerosci.2017.02.003
964
965 Polidori, A., Turpin, B.J., Meng, Q.Y., Lee, J.H., Weisel, C., Morandi, M., Colome, S., Stock, T.,
966 Winer, A., Zhang, J., Kwon, J., Alimokhtari, S., Shendell, D., Jones, J., Farrar, C., Maberti, S.
967 (2006). Fine organic particulate matter dominates indoor-generated PM2.5 in RIOPA homes. *J.*
968 *Exposure Analysis and Environmental Epidemiology* 16: 321-331.
969
970 Pratte P, Cosandrey S, Goujon-Ginglinger C. A scattering methodology for droplet sizing of e-
971 cigarette aerosols. *Toxicology*, 2016;28:537-545. doi:10.1080/08958378.2016.1224956.
972
973 Pubchem. <https://pubchem.ncbi.nlm.nih.gov/compound/Glycerol#section=Vapor-Pressure> .
974 Accessed 2/21/21.
975
976 Public Health England. 2016. *Use of e-cigarettes in public places and workplaces*. London,
977 England: Public Health England.
978
979 Repace, J.L. and A. H. Lowrey. 1980. Indoor air pollution, tobacco smoke, and public health.
980 *Science* 208:464-472.
981
982 Robinson, R. J., E. C. Hensel, P. N. Morabito, K. A. Roundtree. 2015. Electronic cigarette
983 topography in the natural environment. *PLoS ONE* 10(6):e0129296.
984 doi:10.1371/journal.pone.0129296.
985
986 Royal College of Physicians. April 2016. *Nicotine without smoke: Tobacco harm reduction*.
987 London: RCP.
988
989 Ruprecht, A.A., C. De Marco, P. Pozzi, E. Munarini, R. Mazza, G. Angellotti, F. Turla and R.
990 Boffi. 2014. Comparison between particulate matter and ultrafine particle emission by electronic
991 and normal cigarettes in real-life conditions. *Tumori* 100:24-27.
992
993 Ruprecht, A. A., C. De Marco, A. Saffari, P. Pozzi, R. Mazza, C. Veronese, G. Angellotti, E.
994 Munarini, A. C. Ogliari, D. Westerdahl, S. Hasheminassab, M. M. Shafer, J. J. Schauer, J.
995 Repace, C. Sioutas and R. Boffi. 2017. Environmental pollution and emission factors of
996 electronic cigarettes, heat-not-burn tobacco products, and conventional cigarettes. *Aerosol*
997 *Science and Technology* 51(6):674-684. DOI:10.1080/02786826.2017.1300231.
998
999 Saffari, A, N. Daher, A. A. Ruprecht, C. De Marco, P. Pozzi, R. Boffi, S. H. Hamad, Shafer, M.
1000 M., Schauer, J., Westerdahl, D., and Sioutas, C. 2014. Particulate metals and organic compounds

1001 from electronic and tobacco-containing cigarettes: comparison of emission rates and secondhand
1002 exposure. *Environmental Science Processes and Impacts* 16:2259–2267.
1003
1004 Schripp, T., D. Markewitz, E. Uhde, and T. Salthammer. 2013. Does e-cigarette consumption
1005 cause passive vaping? *Indoor Air* 23:25–31.
1006
1007 Sem, G.J., K. Tsurubayashi, and K. Homma. 1977. Performance of the piezoelectric
1008 microbalance respirable aerosol sensor. *American Industrial Hygiene Association*
1009 *Journal*, 38(11):580-588. doi: [10.1080/00028897708984402](https://doi.org/10.1080/00028897708984402).
1010
1011 Sleiman, M., J. M. Logue, V. N. Montesinos, M. L. Russell, M. I. Litter, L. A. Gundel, and Hugo
1012 Destailats. 2016. Emissions from electronic cigarettes: key parameters affecting the
1013 release of harmful chemicals. *Environmental Science & Technology*. 50:9644–9651.
1014
1015 Talih, S., Z. Balhas, T. Eissenberg, R. Salman, N. Karaoghlanian, A. El-Hellani, R. Baalbaki, N.
1016 Saliba, and A. Shihadeh. 2015. Effects of user puff topography, device voltage, and liquid
1017 nicotine concentration on electronic cigarette nicotine yield: measurements and model
1018 predictions. *Nicotine & Tobacco Research*, 150–157. doi:10.1093/ntr/ntu174.
1019
1020 Thermofisher Scientific. <https://www.thermofisher.com/order/catalog/product/TEOM1405>
1021
1022 TSI. 2012. Shoreview, MN, SidePak™ Personal aerosol monitor AM510 user guide.
1023 [http://www.tsi.com/uploadedFiles/Site_Root/Products/Literature/Manuals/](http://www.tsi.com/uploadedFiles/Site_Root/Products/Literature/Manuals/SidePak_AIM510_US_1980456-web.pdf)
1024 [SidePak_AIM510_US_1980456-web.pdf](http://www.tsi.com/uploadedFiles/Site_Root/Products/Literature/Manuals/SidePak_AIM510_US_1980456-web.pdf) (accessed October 10, 2018).
1025
1026 Turpin, B. J., and Huntzicker, J. J. (1995). Identification of secondary organic aerosol episodes
1027 and quantitation of primary and secondary organic aerosol concentrations during
1028 SCAQS. . *Atmos. Environ.*, 29:3527-3544.
1029
1030 USFDA, 2018. Announcement on e-cigarette regulation. Accessed Sept. 13, 2018.
1031 <https://www.fda.gov/NewsEvents/Newsroom/PressAnnouncements/ucm620184.htm> .
1032
1033 Wallace, L., Ott, W., Zhao, T., Cheng, K-C, and Hildemann, L. (2020). Secondhand exposure
1034 from vaping marijuana: Concentrations, emissions, and exposures determined using both
1035 research-grade and low-cost monitors, *Atmospheric Environment X*,
1036 <https://doi.org/10.1016/j.aeaoa.2020.100093> (Accessed 11/19/20)
1037
1038 Williams M, Villareal A, Bozhilov K, Lin S, Talbot P. Metal and silicate particles including
1039 nanoparticles are present in electronic cigarette cartomizer fluid and aerosol. *PLoS One*.
1040 2013;8(3):e57987. doi:10.1371/journal.pone.0057987.
1041
1042 Wright, T.P., C. Song, S. Sears, and M. D. Petters. 2016. Thermodynamic and kinetic behavior
1043 of glycerol aerosol. *Aerosol Science and Technology*, 50:12, 1385-1396.
1044 DOI:10.1080/02786826.2016.1245405.
1045

1046 Zervas. E., Litsiou, E., Konstantopoulos, K., Poulpoulos, S., and Katsaounou, P. 2018. Physical
1047 characterization of the aerosol of an electronic cigarette: impact of refill liquids. *Inhalation*
1048 *toxicology* DOI:10.1080/08958378.2018.1500662.
1049

1050 Zhao T, Shu S, Guo SQ, Zhu Y. Effects of design parameters and puff topography on heating
1051 coil temperature and mainstream aerosols in electronic cigarettes. *Atmospheric Environment*
1052 2016;134:61-69
1053

1054 Zhao, J., J. Nelson, O. Dada, and P. Demokritou. 2018. Assessing electronic cigarette emissions:
1055 linking physico-chemical properties to product brand, e-liquid flavoring additives, operational
1056 voltage and user puffing patterns. *Inhalation Toxicology* 30(2):1-11.
1057 DOI:10.1080/08958378.2018.1450462.

1058 Zhao, T., C. Nguyen, C-H. Lin, H. R. Middlekauff, K. Peters, R. Moheimani, Q. Guo, and Y.
1059 Zhu. 2017. Characteristics of secondhand electronic cigarette aerosols from active human use.
1060 *Aerosol Science and Technology* 51(12):1368-1376. doi: 10.1080/02786826.2017.1355548

1061 Zhao, T., Cheng, K-C., Ott, W.R., Wallace, L.A., and Hildemann, L.M. (2020). Characteristics
1062 of secondhand cannabis smoke from common smoking methods: Calibration factor, emission
1063 rate, and particle removal rate. *Atmospheric Environment* 242:1 December 2020. [https://doi.org/](https://doi.org/10.1016/j.atmosenv.2020.117731)
1064 [10.1016/j.atmosenv.2020.117731](https://doi.org/10.1016/j.atmosenv.2020.117731) (Accessed 2/28/2021)